Optical transitions via the deep O donor in GaP. I. Phonon interaction in low-temperature spectra

B. Monemar and L. Samuelson
Department of Solid State Physics, Lund Institute of Technology, Box 725, S-220 07 Lund 7, Sweden
(Received 27 September 1977)

A detailed investigation of optical transitions via the deep O donor state in GaP is presented, with emphasis on evaluation of the influence of phonons (lattice relaxation) on the spectral behavior of cross sections. Very sensitive purely optical techniques, such as photoluminescence-excitation (PLE) or -quenching (PLQ) measurements on bulk material provide data on optical cross sections which are accurate enough to allow an unambigous evaluation of parameters for phonon interaction in optical transitions. The near-edge part of $\sigma_{p1}^0(h\nu)$ shows clear phonon structure due to two phonon modes $\hbar\omega_1 \approx 19$ meV and $\hbar\omega_2 \approx 48$ meV with linear coupling strengths $\lambda_1 = 1.65 \pm 0.15$ and $\lambda_2 = 1.1 \pm 0.1$, respectively, giving a Franck-Condon shift $\Delta_{FC} = 85 \pm 5$ meV for the O donor in GaP. These values are found to be the same in the O^+ state (σ_{p1}^0 spectra) and in the O^0 state (radiative emission), which justifies the use of a linear model for the electron-phonon interaction. Further, the detailed agreement with the experimental spectra justifies a simple theoretical treatment within the framework of the adiabatic and Condon approximations. A method to separate out the electronic part $\sigma_{el}(h\nu)$ of the optical cross section using the knowledge of the phonon line-shape function has been developed, involving a simple deconvolution procedure of low-temperature experimental data. This electronic spectrum $\sigma_{el}(h\nu)$ is the appropriate one for comparison with theoretical models for photoionization cross sections. A simple effective-mass treatment of such cross sections is developed including effects of wave-function symmetry as well as the real band structure. A fit of this theoretical model to the electronic part of $\sigma_{p1}^0(h\nu)$ gives a threshold energy 1.453 ± 0.002 eV at 1.5 K, which implies a band gap for GaP ~ 14 meV higher than previously established. The spectral behavior of $\sigma_{n1}^0(h\nu)$ at low temperature indicates strong effects of excited states on the O center, extending ≥ 35 meV below the continuum threshold.

I. INTRODUCTION

The detailed physical mechanisms for excitation and recombination of charge carriers via deep impurity levels in the forbidden gap still present one of the major unsolved problems in semiconductor physics. This is in contrast to the relatively good understanding of properties of shallow impurity levels, which has been possible mainly due to the very detailed information available from experiments on, e.g., optical absorption and radiative recombination.[1-4] Such accurate experimental data are to a large extent absent for deep states. Further, for the majority of deep levels recombination of excess carriers is nonradiative. Therefore for the III-V compounds, only in a few cases, such as the GaP,[5-11] and GaAs,[12-19] has some information on electronic states or phononinteraction in transitions via such states been provided from purely optical measurements.

To encourage a proper theoretical description of deep states, considerably more accurate experimental data than have hitherto been available are necessary. One important piece of information to be extracted experimentally is the amount of interaction with phonons (lattice relaxation) in electronic transitions via these deep states. A knowledge of the details in this phonon interaction (which we believe is important for most deep levels in semiconductors) is necessary for the extraction of data for the electronic properties of the center, such as optical cross sections. These in turn give the background for comparison with theoretical models for the potential and wave function for a charge carrier bound in such a state.

In this paper we present a method to evaluate details of the electron-phonon interaction involved in optical transitions via deep centers in the configuration coordinate (CC) approach. It is also shown, that the electronic part of the cross section in optical transitions between a continuum state and a localized deep state in this case can be uniquely extracted from experimental data once the details of the CC phonon contribution is known. The condition for a simple treatment of both these problems is the validity of the adiabatic and Condon approximations and, further, a predominantly linear coupling in the electron-phonon interaction. As an example for experimental data we have chosen the deep GaP:O donor state, for the simple reason that this is one of the few deep levels among the III-V compounds where the identity of the defect is well known (isolated O atom substitutional on P site[5]).

Our low-temperature experimental data for O in p-type GaP clearly show structure due to phonon-

assisted processes in absorption close to the edge. This makes an analysis of the phonon line-shape function for the phonons interacting in the CC mode possible, independent of the luminescence data for the radiative reverse transition from the O level down to the valence band. We find that these two independent experimental determinations of the line-shape function are in excellent agreement. Knowing the details of the CC phonon interaction, it is possible to deduce separately the spectral distribution for the electronic part of the optical cross section by a simple deconvolution of the experimentally measured spectrum. We have derived a simple model within the effective-mass approximation which describes the behavior of the electronic parts of optical cross sections explicitly (using the proper symmetry for impurity and band states). The experimentally deduced electronic spectrum for σ_{p1}^0 in GaP:O is in fair agreement with this simple theory, if details in the real band structure are taken into account. These deconvoluted electronic spectra also serve as an independent test of the strength of the CC phonon coupling, since unrealistic fluctuations in $\sigma_{el}(h\nu)$ are induced by an excessive CC phonon coupling strength. Further, the proper $\sigma_{el}^0(h\nu)$ curve deduced at low temperature serves as a sound basis for the theoretical prediction of the spectral dependence of the total cross section at higher temperatures, which is thus not dependent on any simplified theoretical treatment of $\sigma_{el}(h\nu)$.[20-22] A complication discovered in the course of our detailed experimental investigations is that σ_{p1}^0 for GaP:O is composed of two parts, one of which is temperature dependent.

In the following, we will first (Sec. II) describe the theoretical framework used in the interpretation of experimental data on phonon-assisted deep-level transitions. In Sec. III, there follows a description of the experimental methods used here, with emphasis on reliability of the data obtained. Section IV displays experimental data on σ_{p1}^0 and σ_{n1}^0 for GaP:O at different temperatures below 80 K, and the results are discussed and compared with theoretical calculations. In Sec. V, we discuss some of these new and important observations in somewhat more detail. Section VI gathers some important conclusions arrived at in the previous sections, and outlines future work.

A theoretical derivation of the spectral behavior of the electronic matrix element σ_{el} in the simple effective-mass approximation is presented in Appendix A. In Appendix B is given an example of the deconvolution treatment used to arrive at the actual spectral distribution of the electronic part of the optical cross section. Numerical estimates of different parameters for carrier excitation and recombination process in the GaP:O system, which are crucial to the proper application of the PLE and PLQ methods, are collected in Appendix C.

II. THEORETICAL MODEL FOR OPTICAL PROCESSES VIA DEEP STATES INCLUDING ELECTRON-PHONON INTERACTION

It is a well-known fact that radiative recombination spectra involving deep-lying impurity levels generally involve rather strong phonon coupling, increasing with the depth of the level.[5,14,15,19,23-25] In such spectra a linear interaction with CC phonons is easily observed as a series of equidistant peaks (phonon replicas) for each phonon involved or, if the interaction is very strong, as a broad bell-shaped peak at energies below the purely electronic transitions. In the case of radiative recombination, both initial and final electronic states are usually very well defined within a narrow energy region, greatly facilitating interpretation of the phonon-interaction, since the purely electronic (no-phonon) transition is correspondingly narrow. In absorption processes between a band and a deep level, where either the initial or the final electronic state is within a continuum, a broad range of energy states is available. This gives rise to a broad spectrum even for the purely electronic (no-phonon) transition, and the influence of phonons is not as apparent as in luminescence. The phonons manifest themselves via phonon replicas of the electronic transition σ_{el} also in the absorption spectra, but these replicas may be extremely hard to observe since they overlap considerably.

What is more readily observed is an overall broadening of the absorption spectrum with increasing temperature due to the fact that phonons can be absorbed in the optical transition at elevated temperatures. From an experimental point of view it is therefore desirable to have a theory for the phonon line-shape function (telling the strength of each individual phonon replica) which predicts the broadening of the spectrum at higher temperature.

As already mentioned, the model generally used for a quantitative treatment of electron-phonon interaction in optical transitions involving impurity levels is the so-called configuration coordinate (CC) model.[26-31] In its original form this model is worked out for transitions within localized levels, and it has been successfully applied to such systems as F centers in alkali halides and rare-earth impurities in semiconductors (internal transitions within an ion).[26] However, the general

approximations behind the model, i.e., the adiabatic and Condon approximations, may have a much wider validity, and it is apparent that the model with proper modification can be applied to most optical transitions via impurities in solids. For example, it has been shown by Hopfield, that LO-phonon interaction in radiative transitions involving even shallow states in semiconductors show excellent agreement with the phonon line shape predicted by the CC model.[32] The formalism for the CC model has been worked out a long time ago, and excellent papers exist on the topic,[26-30] for the semiclassical as well as the quantum treatment. Therefore, we shall refer to these treatments, and merely outline some essential steps in the theory for easy reference, as well as point out the assumptions and modifications made in applying the theory to the problem of a band-to-deep-level transition as, e.g., O in GaP. Usually the semiclassical model is used in evaluation of experimental data due to the simple expressions arrived at for the line-shape function. However, the quantum treatment gives considerably more physical insight in evaluating detailed experimental data and is necessary in cases of weak and intermediate electron-phonon coupling as well as at low temperatures. We shall show that the full quantum treatment is not a serious complication of the formalism.

Consider a system of an isolated deep-level defect plus an electron (being either bound to the defect or in a continuum state) plus a number of CC modes interacting with this defect system. We describe the behavior of this system in terms of an adiabatic wave function in the electronic coordinates $\vec{r}$ and nuclear normal coordinates $\vec{Q} = (q_1, \ldots, q_n)$,

$$\psi(\vec{r},\vec{Q}) = \varphi(\vec{r},\vec{Q})\chi(\vec{Q}) = \varphi(\vec{r},\vec{Q}) \prod_i \chi_i(q_i) . \qquad (1)$$

Neglecting the nonadiabatic terms that differentiate φ with respect to $\vec{Q}$, this kind of wave function separates the Schrödinger equation into two coupled equations. One for the electronic part, $\varphi(\vec{r},\vec{Q})$, and one for the vibrational wavefunction for the nuclei $\chi(\vec{Q})$, where the energy eigenvalue for φ enters as adiabatic potential for χ. In calculating the optical transition probability for a transition between state i and f (discrete or continuum states), Eq. (1) gives (written for one normal mode)

$$\begin{aligned} P_{if} &\propto |\langle \psi_f(\vec{r},q)|\, H' |\psi_i(\vec{r},q)\rangle|^2 \\ &\approx |\langle \varphi_f(\vec{r},\tilde{q})|\vec{r}|\varphi_i(\vec{r},\tilde{q})\rangle|^2 \, |\langle \chi_f(q)|\, \chi_i(q)\rangle|^2 \\ &\propto \sigma_{\rm el}\, P_q . \end{aligned} \qquad (2)$$

In this (the Condon) approximation the optical spectrum will be an electronic transition probability, $\sigma_{\rm el}(\tilde{q})$ (where $\tilde{q}$ is the mean q for the vibrational overlap) repeated and weighted by a line-shape function given by the (squared) vibrational overlap integral P_q. [$H' = (e/m)\vec{A}\cdot\vec{p}$ is the optical perturbation Hamiltonian.] To describe a real spectrum we thus need (a) an explicit expression for the dipole integral as a function of photon energy, (b) a solution to the vibrational overlap integral for all normal coordinates q_i active in the optical transition, and (c) a method to sum over all initial and final vibrational states for all modes in (b).

In the following we discuss in somewhat more detail to what extent the two components $\sigma_{\rm el}$ and $P_{\vec{Q}}$ can be deduced from theory, and finally arrive at a procedure for practical use in dealing with experimental spectra.

A. Spectral distribution of the electronic matrix element for an optical transition between a deep level and a continuum

The treatment of this part can naturally be divided into two different problems: (i) How can we get a good description of the electron wave function and the binding potential for the deep discrete state? (ii) What is the proper description of the continuum state if we take the real band structure into account, and how can the disturbance of the band state due to the presence of the localized defect be described?

Clearly none of these problems is solved at present, and, therefore, a detailed theoretical prediction of the whole spectrum for $\sigma_{\rm el}$ is not possible at this stage. Therefore, we shall restrict ourselves to some simple approximate conclusions, which can be drawn for the near-edge problem and can be compared with experiments. Fortunately for the treatment of the electron-phonon interaction, deconvolution methods can be used to deduce the $\sigma_{\rm el}$ spectrum from the experimental σ curve and therefore a theoretical prediction of the detailed shape of $\sigma_{\rm el}$ is not necessary (see Sec. IIC). The dependence of $\sigma_{\rm el}$ on photon energy close to the edge is the simplest problem since there one might assume parabolic bands. For the impurity potential one usually assumes something very localized, but the detailed choice of the potential (δ function, Yukawa, etc.) seems not too critical for calculation of optical cross sections.[33] Therefore a δ-function potential is usually adopted and is the easiest one in calculations. For shallow states the one-band approximation, where the state is derived from wave functions of the same symmetry as the lowest band extremum, is a good approximation, and is extensively used in theory.[34-36] For a deep state this simple approach

fails, and one should consider an impurity wave function with Fourier components from several bands. Furthermore, one is probably even making an approximation if one considers, e.g., a deep donor state as being built up from only conduction-band states; it is quite conceivable that valence-band states would also be admixed in a complete expansion of the localized state wave functions in terms of band states. The simple theories generally employed so far, i.e., the Lucovsky model,[20] and the so-called quantum defect model[21] disregard the importance of the symmetry of the impurity and the continuum state. A proper treatment of the σ_{el} spectrum has to take symmetry effects of the wave function for the bound state into account as well as the real band structure. A detailed account of this problem is beyond the scope of this paper. To illustrate the formalism, we will present a simple treatment for a deep s-like donor state (appropriate for O in GaP), with the assumption of parabolic bands, in Appendix A. The resulting spectral dependence for the photoionization of electrons to a parabolic conduction band haveing a symmetry compatible with the deep donor state is

$$\sigma_n^0(h\nu) \propto (h\nu - E_D)^{3/2}/(h\nu)^3 , \tag{3}$$

i.e., the Lucovsky formula (Ref. 20). For the photoneutralization of the donor state by excitation of electrons from a parabolic valence band (p-like symmetry) we obtain

$$\sigma_p^0(h\nu) \propto (h\nu - E_T)^{1/2}/\{h\nu[E_D^\Gamma + \alpha(h\nu - E_T)]^2\} , \tag{4}$$

where E_D^Γ is the donor binding energy (measured from the Γ minimum), $E_T = E_g - E_D$, and $\alpha = m_v^*/m_c^*$. The different shapes of these two cross sections is illustrated in Fig. 1.

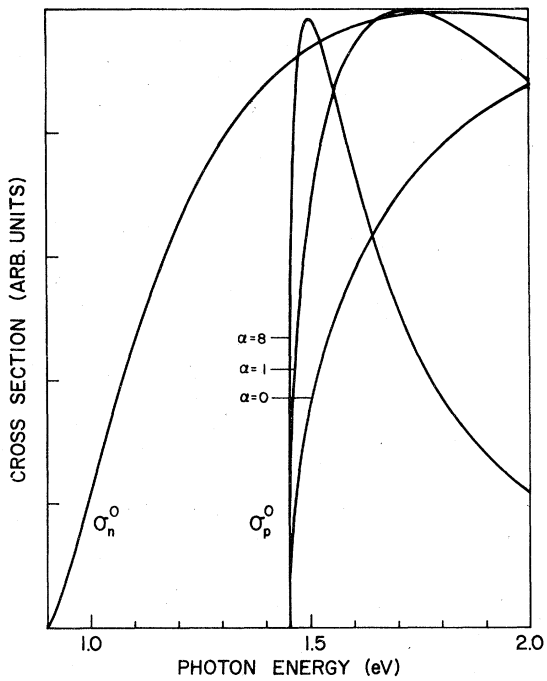

FIG. 1. Spectral dependence of optical cross sections (linear scale) according to the simplified treatment in Appendix A for the electronic part of the transition. The curves plotted are for the O donor in GaP, i.e., $\sigma_n^0(h\nu) \propto (1/h\nu^3)(h\nu - 0.9)^{3/2}$; $\sigma_p^0(h\nu) \propto (h\nu - 1.45)^{1/2}/h\nu[1.4 + \alpha(h\nu - 1.45)]^2$. Three difference curves are shown for $\sigma_p^0(h\nu)$, corresponding to $\alpha = 0$, 1, and 8, respectively. (The case $\alpha = 0$ corresponds to a flat conduction band.)

B. Phonon line-shape function

In the evaluation of the vibrational overlap integral in Eq. (2) (needed to obtain the weighting factor $P_{\vec{Q}}$ for convolution of the zero-phonon cross section, σ_{el}), we assume that the electronic state interacts with symmetric (A_1) localized vibrational modes, e.g., "breathing modes." Because different normal modes are independent, we can write $P_{\vec{Q}}$ as a product of the P_{q_ν}'s for the different normal coordinates $\{q_\nu\}$. Assuming that each mode corresponds to a harmonic potential $E_i(q) = \frac{1}{2}\mu\omega^2 q^2$, the eigenstates ($\chi_{n,i}$) are those of a one-dimensional harmonic oscillator with energy values $\epsilon_{n,i} = (n + \frac{1}{2})\hbar\omega$ and $n = 0, 1, \ldots$ (Fig. 2). In the optical transition we change the charge state of the center, causing, in the linear approximation, a term proportional to q to be added to the potential. This gives the new potential $E_f(q) = E_0 + \frac{1}{2}\mu\omega^2(q - q_0)^2$ with the corresponding energy states $\epsilon_{m,f} = E_0 + (m + \frac{1}{2})\hbar\omega$ (Fig. 2). Hence, the linear approximation results in a shift of the potential parabola minimum to $q = q_0$, E_0 above the initial one but without any change of the phonon frequency (Fig. 2). The validity of this result for the case studied will be discussed in Sec. V. The overlap integral can be calculated as (for $n \leq m$),

$$|\langle\chi_{m,f}(q)|\,\chi_{n,i}(q)\rangle| = e^{-\lambda/2}(n!/m!)^{1/2}\lambda^{(m-n)/2}L_n^{m-n}(\lambda) , \tag{5}$$

where $L_\alpha^\beta(\lambda)$ is the associated Laguerre polynomial,[37] and the parameter λ is defined as

$$\lambda = \mu\omega q_0^2/2\hbar = \tfrac{1}{2}\mu\omega^2 q_0^2/\hbar\omega . \tag{6}$$

Consequently, λ corresponds to the number of vibrational energy quanta the final state is displaced relative to the initial and is thus a direct measure of the phonon coupling strength. At $T = 0$ K only the ground state ($n = 0$) of the initial state is populated in thermal equilibrium, giving the transition probability

$$|\langle\chi_{m,f}(q)|\chi_{0,i}(q)\rangle|^2 = e^{-\lambda}(\lambda^m/m!) \tag{7}$$

i.e., the different replicas have the well-known Poisson distribution often observed in emission.[32,38] For large values of λ, i.e., very strong phonon coupling, this expression approaches a Gaussian distribution observed as bell-shaped emissions in alkali halides and II–VI compounds.[39]

For a finite temperature, the initial states must be weighted by their thermal population factors and a transition from state n to state m will have the probability (for $n \leq m$)

$$P_q(n,m,T) = (1 - e^{-\hbar\omega/kT}) e^{-n\hbar\omega/kT} e^{-\lambda} \times (n!/m!)\lambda^{m-n}[L_n^{m-n}(\lambda)]^2 . \quad (8)$$

$$\sigma(h\nu) = \sum_{n_1=0}^{\infty}\sum_{m_1=0}^{\infty}\cdots\sum_{n_Z=0}^{\infty}\sum_{m_Z=0}^{\infty}\left[\sigma_{el}\left(h\nu - E_0 \pm \sum_{i=1}^{Z}(m_i - n_i)\hbar\omega_i\right)\times\prod_{i=1}^{Z}P_i(n_i,m_i,T)\right] . \quad (9)$$

Here E_0 denotes the zero-phonon energy difference between the two (discrete or continuous) states and the $P_i(n_i,m_i,T)$'s are the probabilities in Eq. (8). This form is convenient for computer calculations of expected experimental curves at different temperatures.

Since, at present, the spectral distribution of the electronic cross section $\sigma_{el}(h\nu)$ cannot be accurately predicted over a large energy range, we shall in such cases use a $\sigma_{el}(h\nu)$ computed from low-temperature data employing a deconvolution method corresponding to Eq. (9) for $T = 0$. With input values for $\hbar\omega_i$ and λ_i, we can express

$$\sigma_{el}(h\nu) = F(\hbar\omega_i, \lambda_i, \sigma(h\nu)) . \quad (10)$$

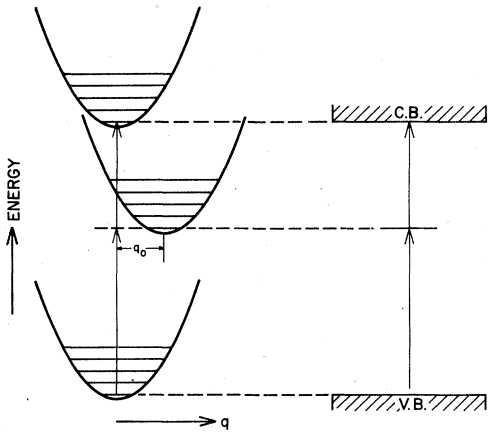

FIG. 2. Configuration coordinate diagram for optical transitions via a deep level in a semiconductor in the linear model for the electron-phonon interaction. The corresponding energy band picture is shown to the right. The thresholds for zero-phonon transitions are indicated by vertical arrows.

C. Explicit expressions for the total optical cross section (including phonon interaction)

With the knowledge of the dipole transition probability between the two electronic states (Sec. II A) and the single-mode vibrational overlap integral (Sec. II B), we can evaluate the total cross section for the transition being either an absorption [(–) sign] or emission [(+) sign]. In an arbitrary case with Z CC modes that couple to the optical transition, we get for the measured total cross section at the temperature T:

It can be shown that this deconvolution procedure is in general unique for the functional form of $\sigma_{el}(h\nu)$, and in Appendix B is given a simple treatment for the general case with N phonon modes. With the aid of a Z-transform technique it is shown that in this case an analytical expression can be obtained for the functional form of F in Eq. (10), as a simple summation over the experimental σ values

$$\sigma_{el}(k) = \sum_{j=0}^{\infty} f_j \sigma_{k-j} , \quad (11)$$

where k is an index for the discrete equidistant experimental points chosen. The σ_{el} thus computed from low-temperature data is the proper choice for comparison with theory for optical cross sections. For the emission case this was illustrated for the GaP:O system in Ref. 40, and in Sec. V we study the absorption of the same system with special attention to the differences between the interpretation of a total experimental cross section and the relevant extracted σ_{el}. This σ_{el} is also in a suitable digital form to generate spectra for higher temperatures, thereby increasing the accuracy in determining the true shift of the electronic threshold with temperature.[41]

III. EXPERIMENTAL TECHNIQUES

The lack of detailed optical data for deep-level transitions is essentially due to experimental difficulties. Straightforward optical transmission measurements on homogeneous material require very large optically perfect samples for accurate measurements of absorption thresholds (α generally below 1 cm^{-1}), but has been attempted in some cases.[11,19] This method is of

course only reliable when other absorption processes in the photon energy region under study can be reduced to a negligible amount, which is at present very difficult in III-V compounds.

Although selective techniques using additional light sources have been attempted in transmission measurements,[42] the bulk of data now available on absorption cross sections for deep impurity levels have been obtained from various measurements on p-n junction or Schottky-barrier structures, such as photocapacitance and photocurrent.[22,43-52] The most significant studies on the III-V-compounds have been done for GaAs and GaP, the center most extensively explored being O in GaP.[22,44,46-48,51,52] The methods involving p-n junctions (or Schottky barriers) are attractive since they, in principle, allow studies of all deep centers in the material, both radiative and nonradiative, provided a reliable p-n junction structure can be prepared. However, the method is generally not selective for different centers with similar positions in the forbidden gap. Further we have observed, that the strong electric field (of the order 10^7 V/m) in a p-n junction can considerably influence the shape of absorption edges obtained by this technique, causing an additional broadening (Fig. 3).

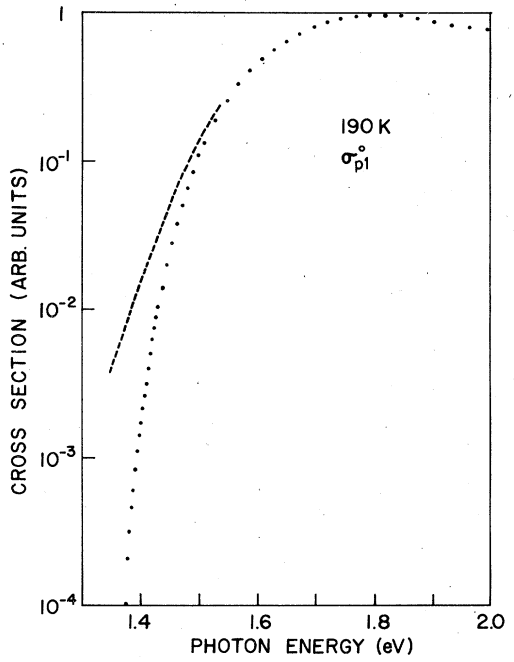

FIG. 3. Comparison between spectral dependence of photoneutralization cross sections $\sigma^0_{p1}(h\nu)$ for O in GaP, measured by two different techniques at 190 K. The dotted line denotes our PLE data, the dashed line is data from photocapacitance measurements by C. H. Henry (Ref. 62).

It has been shown that photoconductivity measurements can give very good sensitivity for deep impurity absorption spectra,[53-57] but the method is not selective for a particular center. Further, all types of electrical measurements, especially those on p-n-junction (and Schottky-barrier) structures are very difficult to carry down to below 50 K. For a detailed evaluation of optical cross sections for deep levels it is very important to have access to reliable experimental data on extrinsic absorption edges down to the very lowest temperature range (say 2 K). Below we shall describe such methods applicable for deep levels with a partly radiative recombination of excess carriers. They provide a selective and very sensitive way of measuring the spectral behavior of optical cross sections for transitions between a deep-level state and continuum band states.

A. PLE method

The measurement of photoluminescence excitation spectra (PLE) is in principle very simple, as can be seen from Fig. 4. In addition to the traditional use of this method in the study of localized defects, it has recently been used successfully to obtain spectral information within the fundamental absorption region of semiconductors.[58,59] In that case, it was difficult to extract absolute values or even the correct spectral variation of the absorption coefficient, except near singularities. In the case of extrinsic PLE spectra, we will show that excellent accuracy can be achieved for the spectral

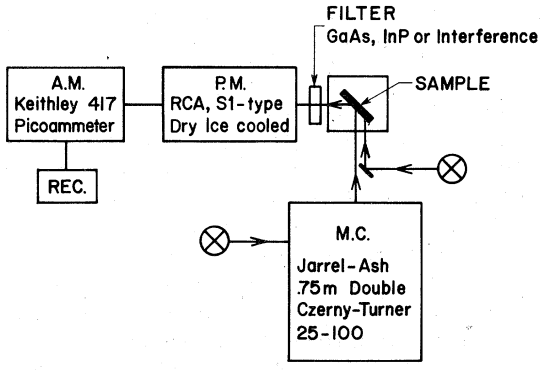

FIG. 4. Schematic picture of the simple experimental setup used to record PLE spectra for the O donor in GaP. Monochromatic light via a double grating monochromator is focused on the sample, and the excited luminescence is detected with an S1 photomultiplier (RCA 7102) via a filter system and recorded on a stripchart recorder as the excitation wavelength is scanned. The only addition necessary for PLQ measurements is the indicated extra light source for primary excitation of the sample.

variation of the absorption coefficient (or the cross section) for impurity to band transitions. The method is fundamentally different from those involving junction structures, i.e., photocapacitance and photocurrent measurements. In the latter case a reverse-biased junction is used to obtain a high-field region, where optical excitations via localized levels can be studied without the influence of recombination (and thermal excitation if the temperature is kept low enough). In the PLE method, we make use of the recombination of excess carriers to detect the absorption processes via deep levels in a bulk sample, indeed a quite different approach. One advantage of the PLE method is its ability to perform measurements down to the very lowest temperatures, where the most accurate information can be obtained on phonon-assisted processes. Further it is selective for different radiative centers. Of course, the method is not directly applicable for centers which have very weak radiative recombination.

To illustrate the kinetics of carriers excitation and recombination via a deep center in relation to PLE measurements, we shall take the specific example of a deep donor state in p-type material. This is relevant to the experimental data on σ_{p1}^0 for O in GaP to be presented below in Sec. IV. In Fig. 5 is shown a picture of the relevant carrier traffic via the O center in p-GaP. Under stationary excitation with photon energies in the range $E_g - E_D < h\nu < E_g$ we have for the total hole capture rate R into the O center, taking even the two-electron state into account,[22]

$$R = \alpha^{-1}L = \sigma_{p1}^0 N_T^+ I - (\sigma_{n1}^0 + \sigma_{p2}^0) N_T^0 I + \sigma_{n2}^0 N_{T2} I + c_{n1} N_T^+ + c_{p2} N_{T2}\,, \quad (12)$$

where L is the radiative emission intensity from the donor down to the valence band (or to shallow acceptor levels at low temperature) and α denotes the radiative efficiency of the hole recombination process from the one-electron state. N_T^+ and N_T^0 are the concentrations of ionized and neutral species, respectively, of the one-electron state, N_{T2} denotes the concentration of two-electron states. Otherwise conventional notations are used.[22,43,60] As will be shown specifically in Appendix C, the traffic via the conduction band as well as the two-electron state can be neglected in p-type material under our experimental conditions. In this case, Eq. (12) reduces to

$$\sigma_{p1}^0 = (\alpha^{-1}L/N_T I)\,, \quad (13)$$

which means that σ_{p1}^0 is directly proportional to the measured luminescence output L for the reverse optical transition. Knowing the radiative efficiency α, the concentration of these centers N_T ($\simeq N_T^+$) and the excitation light intensity, absolute values of σ_{p1}^0 are obtained. A plot of σ_{p1}^0 versus photon energy can be obtained, if I is kept constant and L is observed as a function of $h\nu$ for the excitation light (of intensity I). Here the assumption is made that α does not vary with $h\nu$, which is trivially clear if we assume that the (free and bound) hole concentration is only weakly perturbed by the excitation. For the same reason α should not vary with I for reasonably low flux, which can easily be tested by measuring L as a function of I (Fig. 6). As long as linearity is observed in the L-I dependence (for the extrinsic excitation conditions discussed here), α does not

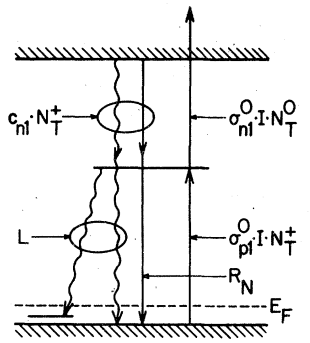

FIG. 5. Schematic picture of the relevant parts of excess carrier excitation and recombination rates in PLE measurements via a deep level.

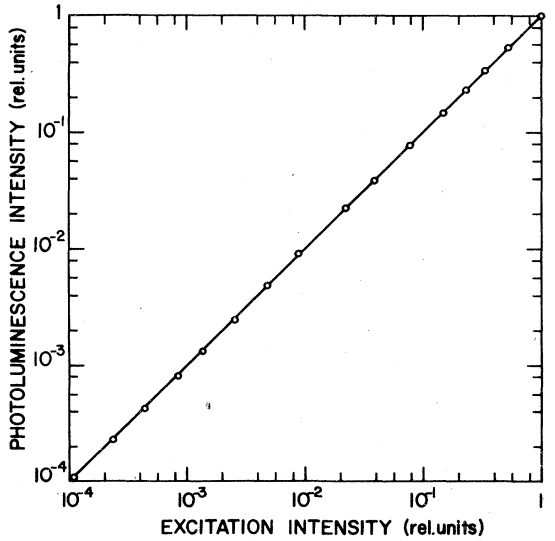

FIG. 6. Logarithmic plot of luminescence intensity for the O related emission vs intensity of excitation light with 1.8-eV photon energy. The maximum excitation intensity employed here was about 10^{15} photons/cm^2 sec.

vary with I (if the temperature is kept constant). Under these conditions it is experimentally more convenient to allow I to vary with $h\nu$, but measure both L and I vs $h\nu$, whereupon σ_{p1}^0 can be calculated from Eq. (13).

The treatment of PLE measurements given here was for radiative transitions from a deep donor down to the valence band. Clearly, the corresponding information about σ_{n1}^0 can be obtained from a similar treatment of radiative capture emission in n-type material. However, other optical methods, such as photoquenching of luminescence, seem to be more suitable for measuring the σ_{n1}^0 transitions in the particular case of GaP:O we have experimentally studied.

B. PLQ method

The PLE method is used to measure the optical cross section for transitions from a deep level to the band that gives a reasonable radiative branch for carrier capture (e.g., donor–valence-band transition). The complementary cross section (in this case for transitions to the conduction band) often has nonradiative carrier capture, but can be studied by another optical technique, the PLQ method (see Fig. 4). As has been shown previously,[61] the spectral distribution of quenching of photoluminescence (PLQ) is (under suitable conditions) proportional to the optical cross section. In Fig. 7, is shown a schematic picture of the relevant carrier traffic via a deep state studied by PLQ. In this case fundamental excitation is used, and a straightforward application of the PLQ technique depends upon the requirement that the center under study is not the main recombination channel for excess carriers.

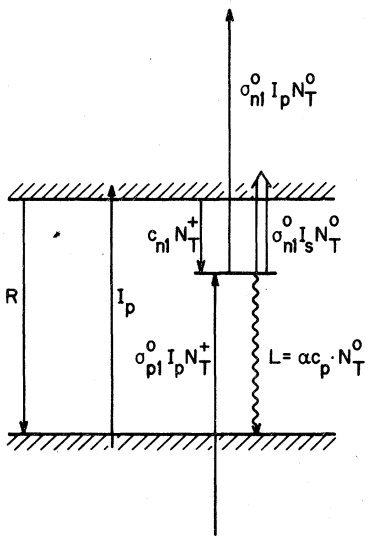

FIG. 7. Schematic picture of the relevant parts of excess carrier traffic in PLQ measurements via a deep level. R denotes the dominating path for recombination (unspecified) for excess carriers.

For specific case of a deep donor with a radiative transition to the valence band (Fig. 7), we have for the intensities L_p without, and L_{p+s} with, secondary excitation of photon energy $E_d < h\nu < E_g - E_d$ in n-type material

$$L_p = \alpha c_p^{(p)} N_T^{0(p)}, \tag{14}$$

$$L_{p+s} = \alpha c_p^{(p+s)} N_T^{0(p+s)}. \tag{15}$$

Here α denotes radiative efficiency of the luminescence. $c_p = \sigma_p v_p p$, where σ_p is the capture cross section for holes to the donor, v_p is the hole thermal velocity, p is the free-hole concentration, and $N_T^{0(p)}$ and $N_T^{0(p+s)}$ denote the density of occupied deep donor states for primary and primary plus secondary excitation, respectively. The quenching ratio Q is most naturally defined as

$$Q = \frac{L_p - L_{p+s}}{L_p} = 1 - \frac{c_p^{(p+s)} N_T^{0(p+s)}}{c_p^{(p)} N_T^{0(p)}}, \tag{16}$$

where (14) and (15) have been inserted. Further, we have under stationary conditions (Fig. 7),

$$\begin{aligned} &\sigma_n^0(h\nu_p) N_T^{0(p)} I_p - c_n^{(p)} N_T^{+(p)} \\ &\qquad = \sigma_p^0(h\nu_p) N_T^{+(p)} I_p - c_p^{(p)} N_T^{0(p)}, \\ &[\sigma_n^0(h\nu_p) I_p + \sigma_n^0(h\nu_s) I_s] N_T^{0(p+s)} - c_n^{(p+s)} N_T^{+(p+s)} \\ &\qquad = \sigma_p^0(h\nu_p) N_T^{+(p+s)} I_p - c_p^{(p+s)} N_T^{0(p+s)}, \end{aligned} \tag{17}$$

where I_p and I_s denote, respectively, the intensities of primary excitation of energy $h\nu_p$ and secondary excitation of $h\nu_s$. Insertion of $N_T^{0(p+s)}$ and $N_T^{0(p)}$ from Eq. (17) into Eq. (16) yields

$$\begin{aligned} Q = 1 - &\frac{c_p^{(p+s)}}{c_p^{(p)}} \frac{\sigma_p^0(h\nu_p) I_p + c_n^{(p+s)}}{\sigma_p^0(h\nu_p) I_p + c_n^{(p)}} \\ &\times \frac{\sigma_n^0(h\nu_p) I_p + \sigma_p^0(h\nu_p) I_p + c_n^{(p)} + c_p^{(p)}}{\sigma_n^0(h\nu_p) I_p + \sigma_n^0(h\nu_s) I_s + \sigma_p^0(h\nu_p) I_p + c_n^{(p+s)} + c_p^{(p+s)}}. \end{aligned} \tag{18}$$

This can be reduced to

$$Q = \beta \sigma_n^0(h\nu_s) I_s + \beta \frac{(c_n^{(p)} - c_n^{(p+s)})(\sigma_n^0(h\nu_p) I_p + c_p^{(p)})}{\sigma_p^0(h\nu_p) I_p + c_n^{(p)}}, \tag{19}$$

where

$$\beta = \frac{1}{[\sigma_n^0(h\nu_p) + \sigma_p^0(h\nu_p)] I_p + (c_n^{(p+s)} + c_p^{(p+s)}) + \sigma_n^0(h\nu_s) I_s},$$

if we assume that $c_p^{(p)} - c_p^{(p+s)} = 0$. The last assumption is true if the center under study is not

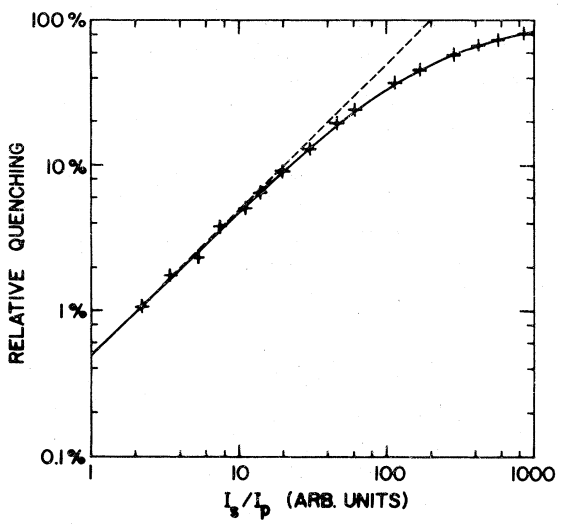

FIG. 8. Comparison between the theoretical expression [Eq. (20)] for PL quenching ratio Q (solid line) and experimental data (+) for different values of the ratio of secondary and primary excitation intensities I_s/I_p.

a dominant recombination center. For such a center we may assume negligible change in concentration of minority carriers (holes) as well as majority carriers (electrons) on application of the secondary light in the above mentioned restricted energy range. This means that in the second term of Eq. (19), $c_n^{(p)} - c_n^{(p+s)} \approx 0$. We therefore arrive at a convenient linear relationship between Q and I_s, i.e.,

$$Q \approx \beta \sigma_n^0(h\nu_s) I_s , \tag{20}$$

if β is constant.

The validity of Eq. (20) depends experimentally on the chosen ratio I_s/I_p, and, as is shown in Fig. 8 for n-type O-doped GaP, a suitable choice of this ratio perfectly validates Eq. (20). Thus, over a small energy interval, it is possible to scan Q vs $h\nu$ and accurately record $\sigma_n^0(h\nu_s)$. Since the validity of Eq. (20) restricts the excitation intensities, the PLQ method is usually less sensitive than the PLE method described above. By keeping Q constant, it has been possible to measure nearly four orders of magnitude of the rise of σ_{n1}^0 in GaP:O, which is far better than previously reported with other methods.

In application of the above PLQ method to the O donor in GaP, the presence of the two-electron state must be considered. In Appendix C, we elaborate on this point, and show that under suitable conditions Eq. (20) is still valid for evaluation of $\sigma_{n1}^0(h\nu)$.

IV. EXPERIMENTAL RESULTS FOR GaP:O

With the experimental technique described in the previous section a detailed study was carried out on the photoneutralization cross section σ_{p1}^0 in GaP:O in the temperature range 1.5 to 300 K (PLE measurements). In addition, PLQ data were collected for the σ_{n1}^0 -transition, in order to achieve accurate optical data for both cross sections from bulk material. In this paper, we concentrate on the data collected at the very lowest temperatures, where the details of the phonon interaction problem are most clearly displayed. Phonon broadening at higher temperatures, as well as other effects of temperature on optical cross sections, are discussed separately.[41]

In Sec. IV A below we display the PLE and PLQ data, compared with data from the radiative emission from the O center. In Sec. IV B the phonon-interaction parameters deduced from these data are used to obtain the purely electronic part of the cross section, via deconvolution of experimental spectra. It should be pointed out that the spectra obtained are representative of several different crystals from different sources, where the major p dopant was Zn, but in some cases C (crystals were from three sources: IBM T.J. Watson Center, Ferranti Ltd., United Kingdom and those we grew ourselves in Lund).

A. PLE and PLQ measurements at low T

In Fig. 9 is shown in a logarithmic plot the overall appearance of the σ_{p1}^0 curves, measured over nearly five orders of magnitude with 1.5-meV spectral resolution. (Access to a more sensitive photomultiplier than the S1 type employed here would increase this sensitivity considerably.) The curve rises sharply from the threshold energy of about 1.44 eV, peaks at about 1.81 eV and decreases continuously up to 2.2 eV. Measurements at higher photon energies are difficult to evaluate for σ_{p1}^0 because the fundamental absorption invalidates the simple treatment in Sec. III A. The curve looks smooth, as one would expect from a convolution of any broad electronic spectrum with a reasonable amount of phonon interaction involved. Since even the simplified models for the purely electronic transitions (Sec. II A) predict smooth curves if effects from the band structure are not drastic, no judgement on the influence of phonons on the spectral shape can be drawn from a gross inspection of curve such as Fig. 9. Clearly, the relevant details in the phonon interaction are expected to show up most easily close to the edge. A careful study was therefore made of the near-edge region at 1.5 K. The onset

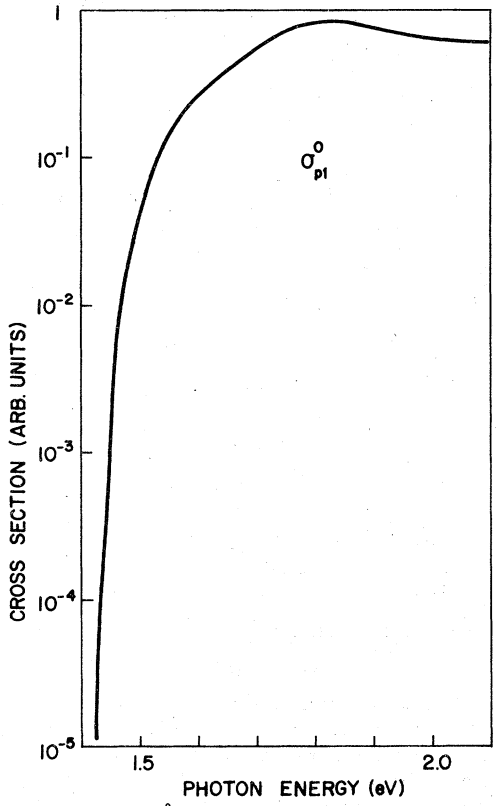

FIG. 9. Plot of $\sigma^0_{p1}(h\nu)$ for 0 for GaP at 30 K from PLE measurements on the O-related DA-pair emission. Note that five orders of magnitude are measured of the absorption edge with about 1.5-meV spectral resolution.

of the signal related to σ^0_{p1} occurred at 1.442 ± 0.002 eV in the samples studied (Fig. 10), and the first part of σ^0_{p1} has the appearance of a tail with a photon energy dependence like $(h\nu - E)^\alpha$ where $\alpha \geq 1$. A drastic rise in σ^0_{p1} occurs at about 1.452 eV and in the energy region 1.454–1.467 eV the curve has an energy dependence $(h\nu - E)^\beta$ where $\beta \simeq \frac{1}{2}$. At higher photon energies a number of phonon replicas of this edge region are observable up to 1.55 eV, essentially due to the occurrence of the steep edge around 1.452 eV. The first replica of this edge occurs at 1.471 ± 0.001 eV, a second occurs at about 1.491 ± 0.002 eV which is somewhat obscured by the third at 1.500 ± 0.002 eV. The most prominent replicas at higher photon energy occur at 1.519 ± 0.001 eV and 1.539 ± 0.001 eV (Fig. 10). Thus the electronic (no-phonon) part of the σ^0_{p1} spectrum seems to be observable up to 1.47 eV. Above this photon energy the CC phonon interaction dominates the spectral shape.

It is of interest to compare the experimental results on $\sigma^0_{p1}(h\nu)$ from Fig. 10 with spectral results from the low-temperature DA-pair emission on the same sample. Such a comparison is shown in Fig. 11, where the derivative $\sigma^0_{p1}(h\nu)$ spectrum is shown in order to display the similarity with emission data. In emission we have a rather narrow electronic peak,[40] and evaluation of the strengths of the two phonon modes $\hbar\omega_1 \approx 19$ meV and $\hbar\omega_2 \approx 48$ meV is fairly accurate

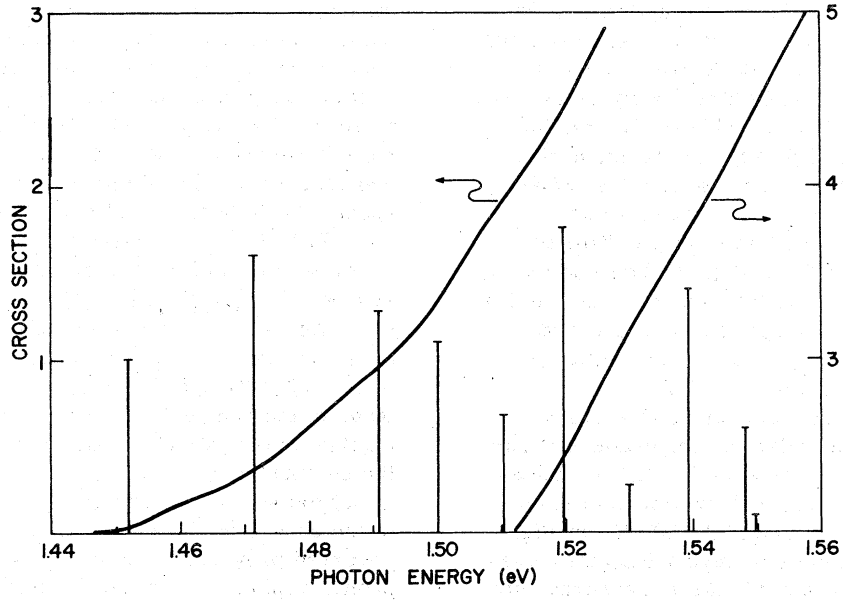

FIG. 10. Detailed linear plot of $\sigma^0_{p1}(h\nu)$ for GaP:O at 1.5 K. The right-hand part of the curve is displaced vertically for clarity. The expected position and relative strength of each phonon replica of the feature at 1.452 eV is indicated by vertical bars.

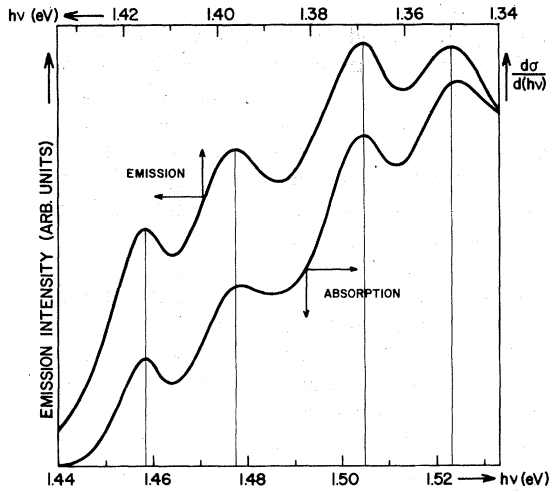

FIG. 11. Comparison between the PL emission intensity spectrum (upper curve, linear scale) and the derivative spectrum ($d\sigma^0_{p1}/dh\nu$) of the absorption curve (linear scale) for GaP:O at 4 K, which strongly indicates that the CC phonon energies are the same in emission as in absorption.

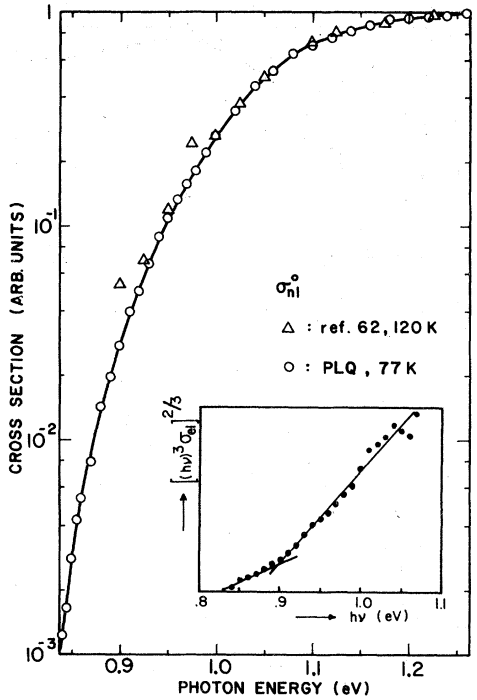

FIG. 12. PLQ spectrum for $\sigma^0_{n1}(h\nu)$ in GaP:O at 77 K compared to photocapacitance measurements from Ref. 62. The insert shows the resulting $\sigma^0_{el,n1}$ of an approximate deconvolution at 77 K plotted to linearize the theoretical expression in Eq. (3).

via stepwise deconvolution (Ref. 40 and Appendix B), the quoted values being $\lambda_1 \approx 1.65 \pm 0.15$ and $\lambda_2 = 1.1 \pm 0.1$. From Fig. 10 it is apparent that the observed steps can be assigned as phonon replicas of the 1.452-eV edge with these same phonons: 1.471 eV ($\hbar\omega_1$), 1.491 eV ($2\hbar\omega_1$), 1.500 eV ($\hbar\omega_2$), 1.519 eV ($\hbar\omega_1+\hbar\omega_2$), and 1.539 eV ($2\hbar\omega_1+\hbar\omega_2$).

In the bottom of Fig. 10 it is also indicated where we expect phonon replicas of the 1.452-eV edge and their r relative strengths, according to emission data.[40] The two extra steps expected below 1.55 eV (around 1.51 eV and 1.53 eV) are considerably weaker and therefore not as apparent in the experimental curve. These observations from Figs. 10 and 11 justify the statement that $\hbar\omega_1$ and $\hbar\omega_2$ have the same energies (say ±5%) in absorption and emission. The coupling strengths λ_1 and λ_2 in absorption are difficult to evaluate directly from Fig. 10, because the spectral behavior of the background is not obvious. However, such an attempt to evaluate λ_1 and λ_2 gave values which within 20% agreed with those stated above from emission data.

The PLQ technique has been used to study $\sigma^0_{n1}(h\nu)$ in GaP:O at different temperatures. The method is not as sensitive as the PLE measurement for σ^0_{p1}, but three to four orders of magnitude could be measured at $T < 200$ K. In Fig. 12 is shown an example of such a PLQ measurement, compared with a σ^0_{n1} curve measured with photocapacitance technique,[62] where the difference in sensitivity is evident. Unfortunately, the sensitivity of the experiment dropped below 60 K, so that we have been unable to obtain any good data revealing details of the "camel's back" structure in the conduction band.[63] There are many reasons why a detailed evaluation of the spectral behavior of the photoionization cross section close to the continuum edge will be difficult for the O donor. One obvious reason is clearly observed in Fig. 12, namely a strong contribution of excited states to the $\sigma^0_{n1}(h\nu)$ spectrum. The vibronic broadening of $\sigma^0_{n1}(h\nu)$ up to 77 K can be neglected for the upper two to three orders of magnitude, and therefore the strong tail below 0.9 eV in Fig. 12 must be due to excited states contributing to the electronic cross section. In fact, the lowest measured point of $\sigma^0_{n1}(h\nu)$ at 77 K falls below 0.840 eV, which leads to the conclusion that the optically active excited states extend at least ~35–40 meV below the continuum edge (at ~0.89 eV at 77 K). This is not too surprising, since excited states close to the conduction band are expected and have been observed previously for the O center.[64] The phonon replica of this tail region will overlap the continuum edge, which effectively masks any possible structure in this edge. The photo-

ionization continuum is expected to have approximately a $(h\nu - E)^{3/2}$ dependence close to the edge [Eq. (3)], and replicas of such an energy dependence would be extremely hard to observe even in the absence of excited states.

B. Deconvoluted spectra for $\sigma_{el}(h\nu)$

The spectral distribution of the electronic matrix element σ_{el} is obtained from Eqs. (B12) and (B18) applied to experimental data. A typical spectrum for $\sigma^0_{p1,el}(h\nu)$ obtained in this way (at 4 K) is shown in Fig. 13 for phonon parameters $\lambda_1 = 1.65$, $\hbar\omega_1 = 19$ meV, $\lambda_2 = 1.1$, $\hbar\omega_2 = 48$ meV. There are at least three important new observations one can obtain from Fig. 13: (i) Apart from the tail region below 1.452 eV, the rise in $\sigma_{el}(h\nu)$ curve for $h\nu < 1.5$ eV can essentially be described as $\sigma_{el}(h\nu) \sim (h\nu - \epsilon_0)^{1/2}$, in good agreement with Eq. (4). (This will be discussed in more detail under V B.) (ii) The main peak of $\sigma_{el}(h\nu)$ occurs at about 1.73 eV with a half width of about 0.2 eV. (iii) A monotonic decrease in $\sigma_{el}(h\nu)$ occurs for photon energies >1.8 eV.

The $\sigma^0_{p1,el}(h\nu)$ spectrum for photon energies close to the edge is shown in more detail in Fig. 14. To make Eq. (A14) as realistic as possible within this framework we have computed the density of states $\rho_v(h\nu)$ for the valence band using the $\vec{k}\cdot\vec{p}$ method and a full 6×6 matrix for the valence-band wave functions, the resulting curve is shown in Fig. 15. This density-of-states curve does not show any appreciable rise in the contribution from the light-hole band in the region $\frac{2}{3}\Delta_{so}$ from the edge,[65] and therefore this effect cannot explain the apparent rise in the deconvoluted curve just below 1.50 eV. The fit to Eq. (A14) is surprisingly good close to the edge and can be used to evaluate a value of the σ^0_{p1} threshold as 1.453 ± 0.002 eV at 1.5 K. The tail below this value cannot be fitted within this framework of parabolic bands; possible reasons for this will be discussed below (Sec. V B). The deconvoluted $\sigma^0_{p1,el}(h\nu)$ spectrum also does show a peak in the energy region $h\nu$

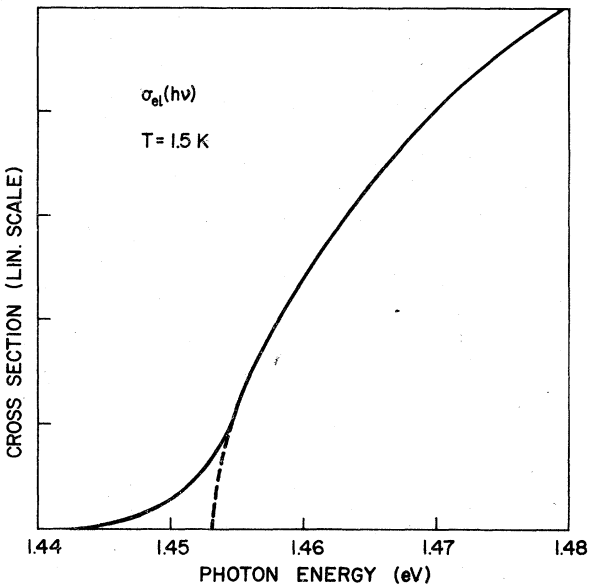

FIG. 14. Deconvolved curve $\sigma_{el}(h\nu)$ (solid line) from $\sigma^0_{p1}(h\nu)$ measured at 1.5 K in the near-edge region. The slashed curve (dashed line) is a simplified theoretical curve according to Eq. (A14) with a realistic density of states $\rho_v(h\nu - E_T)$ and $\alpha = 0$ corresponding to a flat conduction band.

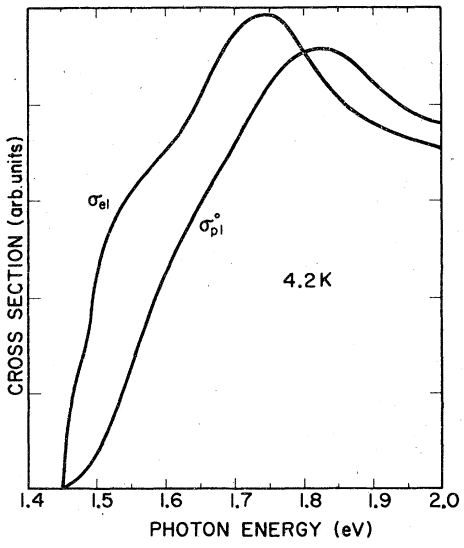

FIG. 13. Comparison between the total experimental cross section $\sigma^0_{p1}(h\nu)$ at 4 K and the deconvolved electronic spectrum $\sigma_{el}(h\nu)$ (linear scale).

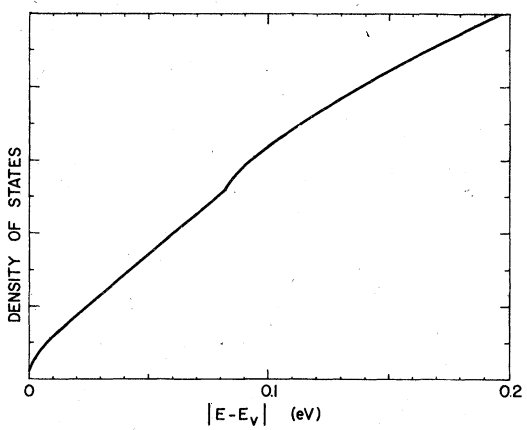

FIG. 15. Valence-band density of states in GaP calculated by a 6×6 matrix $\vec{k}\cdot\vec{p}$ method using the set of valence-band parameters from Ref. 86.

≈ 1.55 eV, in agreement with Eq. (4). As will be shown in more detail in the second part of this investigation,[41] σ^0_{p1} is actually composed of two different contributions, of which the near-edge part peaking at ~1.55 eV is temperature dependent, and decreases in magnitude with increasing temperature. The broad peak in $\sigma^0_{p1,\mathrm{el}}(h\nu)$ at about 1.73 eV in Fig. 12 is due to the temperature-independent part of $\sigma^0_{p1,\mathrm{el}}(h\nu)$, which will dominate at not too low temperatures.[41] The presence of these two parts is clearly visible already in the original PLE data (Fig. 9) and is apparent also in photocapacitance curves measured at 77 K.[66]

To deconvolute σ^0_{n1} we face the problems that excitation to excited states might have different parameters for phonon coupling than continuum excitations and that the deconvolution formalism is written for zero temperature while our data are for 77 K. However, the result of such an attempt to deconvolute σ^0_{n1} gives the $\sigma_{\mathrm{el},n1}$ that is shown in the insert of Fig. 12. The data are plotted as $[(h\nu)^3\sigma_{\mathrm{el}}]^{2/3}$, to test Eq. (A13) for a (dipole forbidden) photoionization process. The almost linear region above the threshold at ~0.89 eV supports this theory and the deviation for energies below 0.89 eV is expected for transitions involving excited states.

V. DISCUSSION

A. Phonon interaction in optical processes via deep levels

In previous investigations on impurity properties it has been customary to neglect totally the presence of phonon cooperation in the evaluation of spectral dependences of cross sections, and these have been treated as being of purely electronic origin (Refs. 13, 16, 17, 20, 21, 36, 42, 44, 45, 50, 51, 53, 56, 61, and 67–72). This in spite of the well-known fact that phonons (relaxation effects) are important and have a strong influence in all cases of radiative transitions observed for deep levels in semiconductors.[12,23–25] In a few cases phonons have been taken into account in such analyses, but the evaluation of parameters is done in an oversimplified manner.[11,22,73] To gain real insight into relaxation phenomena connected with change of charge state for a defect, the energy and coupling strength of each vibrational mode taking part in electronic transitions has to be known. We have demonstrated that this information can, at least in some cases, be obtained from simple optical measurements on bulk material at very low temperatures. The analysis of data has to be based on a quantum treatment if these details are to be extracted. The basic assumptions used in our evaluation are that the adiabatic and Condon approximations hold, further that the linear term dominates in the electron-phonon interaction. The adiabatic approximation is believed to be excellent for deep centers,[28,74] while it may break down for shallow centers where phonon energies are of the same order of magnitude as the electronic binding energy. The validity of the Condon approximation has previously been questioned for such transitions.[11] If the electronic matrix element (or the effective field[28]) depends strongly on q, a proper separation in Eq. (2) will be more complicated. For optical transitions between electronic levels, this non-Condon correction is expected to be only of the order E(vibration)/E(electronic). The errors introduced by the Condon approximation will give uncertainties in the deconvoluted spectra far away from the zero-phonon part, while the approximation is expected to be very good for the first replicas. Our data from deconvolution and convolution of emission and absorption spectra confirm that the corrections to the separation in Eq. (2) are minor effects. In other cases, like scattering processes, where the interaction Hamiltonian is a strong function of the inter-ion separation, the non-Condon correction will be a first-order effect. Further, nonadiabaticity and non-Condon terms (that in the optical transitions are second-order corrections) can not be omitted in treatments of multiphonon capture.[26,62] Here, the nonadiabatic terms [involving $(\partial\varphi/\partial q)$], are those that give the coupling between the, otherwise, orthogonal states. For capture close to the crossover point, E(phonon)/E(electronic) can be a dominant factor for the transition probability.

The vibrational modes that take part in the optical transitions studied here in the GaP:O-system consist of two sharp modes with energies 19 ± 1 meV and 48 ± 1 meV, i.e., they are resonant with the acoustic and optical phonon bands, respectively. At least for the 19-meV mode, the rapidly relaxing excited states seem to be lifetime broadened by, typically, ~3 meV.[40] Phonon emission and absorption ($\Delta n \neq 0$) processes in optically induced electronic transitions require a coupling of the electronic system to the vibrational coordinate because of the orthogonality properties of nondisplaced oscillators. Such modes are expected to be different from the infrared active local modes for the center,[75,76] where coupling of an electronic wavefunction to the vibrational coordinate does not enter the transition probability.

An important observation is that the energies of the phonons coupled to the different charge states of O (i.e., emission versus absorption) are equal within experimental uncertainty (say 5%). This is not consistent with the model used to interpret measurements of capture cross sections at ele-

vated temperatures for the same center, where a shift of 22% in phonon energies between different charge states has been postulated to explain a factor ~10^9 difference between experimental data and predictions from the theory of multiphonon emission.[52,62,77] Apparently mechanisms other than mode softening have to be invoked to explain such large discrepancies.

As pointed out previously the broadening effects caused by a high electric field make conventional methods employing $\bar{p}n$ junctions or Schottky barriers unsuitable for revealing the details in the vibrational coupling. Optical measurements on bulk materials of the kind presented here are therefore invaluable as a complement to the conventional measurements, even though their applicability is restricted to a much smaller class of defects due to the requirement of a partly radiative recombination branch. Furthermore, even in cases where optical data do not reveal any phonon structure, the formalism of deconvolution of low-temperature spectra developed here gives a valuable tool for estimating an upper bound for the strength in phonon coupling, assuming reasonable phonon energy. With the aid of such a σ_{el} spectrum obtained from deconvolution of experimental data taken at the lowest possible temperature, broadening effects at higher temperatures can be accurately predicted and compared with experiment. The formalism developed is in this sense a universal method to study phonon coupling strengths as well as electronic properties of deep levels.

B. Evaluation of electronic cross sections for deep-level transitions

As has been shown explicitly in Sec. IV B for GaP:O, the deconvoluted spectrum for optical cross sections is a unique solution from which reliable data for the electronic spectrum of the optical transition can be extracted. The CC phonons (i.e., the lattice relaxation) can be separated from the problem in this way. If momentum conserving (MC) phonons are important in the optical transition,[78] they may be naturally incorporated in the formalism for the electronic transition.[40] In the case of GaP:O described here, transitions near Γ in the Brillouin zone dominate, and the MC phonons can thus be neglected. A comparison between our deconvoluted curves and the experimental σ^0_{p1} curve (Fig. 13) reveals that even for a moderate relaxation, as for the one-electron O state in GaP, it makes no sense at all to fit models for the electronic cross sections directly to experimental data. Since the spectral behavior of optical cross sections is the most valuable test of theoretical calculations based on specific assumptions on bound electron potential and wave function, this point is crucial. One can safely predict that relaxation of at least the same order of magnitude as found for O_1 in GaP is present for most deep levels in GaP and GaAs, and therefore for these materials a deconvolution treatment seems to be mandatory in evaluation of optical cross sections. The role of relaxation effects for deep levels in elementary semiconductors such as Si is unclear. Most authors believe such effects can be neglected,[79] but some detailed spectral data on Si:Co have been interpreted in terms of phonon replicas.[57] The most recent data on the Si:Au center also show evidence for lattice relaxation.[80]

An interesting new result that has appeared from our detailed investigations of the near-edge part of $\sigma^0_{p1}(h\nu)$ in GaP:O is that the leading part of the threshold indicates a value of 1.453 ± 0.002 eV for the distance between the O-donor level and the valence band at 1.5 K. The shallow donor binding energies for GaP were established relatively early to within ~1 meV via ir transmission measurements.[81] The binding energy of the deep O donor was therefore known with the same accuracy, since it has been obtained for DA-pair spectra in comparison with shallow donors.[82] (The donor-acceptor distances are of course known with excellent accuracy from these same DA-pair analyses.[2,24,82]) Recently, an upward revision of all donor binding energies with three to four meV has been suggested,[83,84] when the "camel's back" behavior of the GaP conduction band is included in the analysis of donor spectra. Thus the O-donor binding energy at 1.5 K is about 0.899 ± 0.001 eV, indicating a band gap of 2.352 ± 0.003 eV for GaP at 1.5 K, about 14 meV higher than reported from original transmission data.[85] Since the excitonic band gap is well established,[85] this would also mean a drastically increased value for the free exciton binding energy in GaP ($E_{ex} \approx 24 \pm 3$ meV instead of the original value 10 ± 1 meV[85]). It is interesting to note that this new value of E_{ex} comes closer to the theoretical estimate of 18.5 meV from effective-mass theory[86] (neglecting possible influence of the "camel's back" in the conduction band).

A comparison of these results with earlier data[82,87,88] gives a somewhat confusing picture. There seems to be some controversy about the acceptor binding energies. Preliminary data from ir absorption on heavily p-doped samples[87] indeed indicate values that are about 8 meV higher than those previously established,[3] although it has to be admitted that these data have been obtained via a subtraction of a very strong background con-

taining phonon structure. On the other hand recent measurements on PLE spectra for a discrete DA pairs indicate that the earlier lower values are essentially correct.[88] This situation illustrates, that the energy spectra of excited states of acceptors in GaP are not well understood at present.[89]

In the absence of direct measurements of the free exciton binding energy, a higher band gap of GaP thus remains as one natural explanation of the σ_{p1}^0 data; in that case the tail below 1.452 eV has to be ascribed to some unspecified broadening mechanism. On the other hand, at the detection limit of our setup, the tail extends down to 1.442 ± 0.002 eV, which is where expected according to the original value of the band gap. We feel the scatter in this edge ± 0.002 eV is real between different samples (the monochromator repeatability is better than that). Thus, if the old value of the electronic threshold[82,85] $E_g - E_d$ is correct, there must be some interaction present to severly distort the edge region of the electronic spectrum from what is expected based on parabolic bands close to the edge (we believe the expected terms linear in k for the valence-band top[90] are too small in GaP to account for such a distortion).

A possible source for a shift of the absorption edge in transitions between a band and an impurity level that should be important is the Coulomb interaction E_C between the studied impurity and other charged atoms. In the σ_p^0 process we photoneutralize oxygen atoms which interact with ionized acceptors (in p-type material). The magnitude of this interaction that shifts the donor level by $E_C(R)$ is determined by the statistical distribution between different donor-acceptor distances R similar to the problem in DA-pair recombination.[2,82] This effect, which will be discussed in detail separately,[91] suggests that the σ_p^0 threshold will be broadened and effectively shifted to higher energies by $\langle E_C \rangle - E_A^*$. Here $\langle E_C \rangle$ corresponds to the peak in the distribution function for different distances for charged donor-acceptor pairs, and E_A^* is a correction for transitions into excited bound hold states induced by the Coulomb field of the acceptor.[91] The resulting shift induced by these different Coulomb effects are estimated to be ~2 to 3 meV and might thus explain only a minor part of the discrepancies between the position of the main edge at 1.453 eV and the old value for $E_g - E_D$.[82,85]

VI. CONCLUSIONS

We have presented, for the first time, a detailed experimental study of the influence of lattice relaxation on optical transitions involving a deep state in a III-V semiconductor (O in GaP). The study was made possible by employing novel purely optical techniques of high sensitivity to measure optical cross sections for the particular center under study. E.g., we have observed in detail both emission properties of the GaP:O center via luminescence, and optical absorption via the PLE method, both methods selective for the particular center and useful down to the lowest temperature where all spectral details of importance for a complete description are resolved. The experimental results for GaP:O evaluated with a realistic theoretical model have provided novel physical insight into the details of phonon interaction in optical transitions via deep states. It is demonstrated that a detailed knowledge of this problem is a prerequisite for an adequate discussion of the behavior of the electronic part of the optical cross sections for such a deep state.

The configuration coordinate model extensively used for internal optical transitions within localized defects is shown to be very useful for a description of lattice relaxation via coupling to localized phonon modes that do not contribute momentum in the optical transition. We have employed a simple quantum treatment of the vibronic problem which successfully describes observed experimental results for GaP:O in both radiative emission and optical absorption from the valence band. The main assumptions necessary for this treatment are the adiabatic and Condon approximations, both shown to be good for this center. The relaxation properties in optical transitions via the one-electron state in GaP:O can be completely described with two narrow phonon modes of energies $\hbar\omega_1 = 19 \pm 1$ meV, $\hbar\omega_2 = 48 \pm 1$ meV and coupling strengths $\lambda_1 = 1.65 \pm 0.15$ and $\lambda_2 = 1.1 \pm 0.1$, giving a total Franck-Condon shift $\Delta_{FC} = 85 \pm 5$ meV. We have also developed a deconvolution method for experimental optical spectra by which these can be relieved from the influence of CC phonon interaction. The σ_{el} spectrum for the electronic part of the optical transition, can thus be extracted for adequate comparison with theoretical predictions. Evaluation of such spectra also provide the only reliable basis for prediction of the spectral shape of optical cross sections at higher temperature due to phonon broadening, since no simplifying theoretical models have to be assumed for σ_{el}. For comparison with deconvoluted data for $\sigma_{p1,el}^0(h\nu)$ for GaP:O we have used a simple theoretical treatment that takes into account the symmetry properties of the deep state as well as the continuum states. This theory predicts a spectral behavior $\sigma_{p1}^0 \sim (h\nu - E_T)^{1/2}$ close to the threshold, in good agreement with experimental data with a 1.5-K threshold energy of 1.453

± 0.002 eV. In the explanation of a ~14-meV upward shift of the spectrum compared to the expected position, a higher value for the band gap E_g as $E_g = 2.352 \pm 0.003$ eV at 1.5 K is considered.

The fact that the shape of $\sigma^0_{p1,\mathrm{el}}(h\nu)$ is entirely different from the experimental $\sigma^0_{p1}(h\nu)$ curve leads to the important conclusion, that the usually attempted fit of model calculations for $\sigma_{\mathrm{el}}(h\nu)$ directly to experimental spectra is meaningless in cases of non-negligible lattice relaxation. It turns out that $\sigma^0_{p1}(h\nu)$ for O in GaP is composed of two overlapping contributions, one of which has a temperature-dependent strength.

ACKNOWLEDGMENTS

We would like to thank A. Baldereschi, J. Bernholc, H. G. Grimmeiss, L-Å. Ledebo, U. Lindefelt, T. N. Morgan, and S. T. Pantelides for valuable discussions during the course of this work. J. W. Cooley made a significant contribution in the development of the deconvolution method described. We also gratefully acknowledge the supply of GaP material from A. R. Peaker at Ferranti Ltd., United Kingdom and T. N. Morgan at IBM Thomas J. Watson Center.

APPENDIX A: SIMPLE THEORETICAL MODEL FOR PHOTOIONIZATION AND PHOTONEUTRALIZATION CROSS SECTIONS FOR A DEEP STATE

We will use as an example a deep donor with a bound electron state which, in the Kohn formalism,[34,92] can be deduced from the conduction-band Bloch states, $|c,\vec{k}\rangle = u_{c,\vec{k}}(\vec{r})e^{i\vec{k}\cdot\vec{r}}$ as

$$\psi_D(\vec{r}) = \sum_{\vec{k}} A_D(\vec{k})|c,\vec{k}\rangle \tag{A1}$$

(including more than one band is a trivial extension of the treatment below and is of course necessary for a deep state). We want to estimate photoionization and photoneutralization cross section for transitions between this state and the two bands. The following Golden Rule expression for a discrete-continuum transition, where $\rho(E_l)$ is the density of states in the continuum state, $|l,\vec{k}\rangle$, is obtained

$$W = (2\pi/\hbar)(\langle l,\vec{k}|H'|\psi_D\rangle)^2\rho(E_l)\,. \tag{A2}$$

Here the perturbation Hamiltonian $H' = (e/m)\vec{A}\cdot\vec{p}$ includes the vector potential $\vec{A}$ and the momentum operator $\vec{p} = -i\hbar\vec{\nabla}$.

Inserting (A1) into (A2) yields

$$\sigma \propto \frac{1}{h\nu}\left(\sum_{\vec{k}} A_D(\vec{k})\langle l,\vec{k}|-i\hbar\vec{\nabla}|c,\vec{k}\rangle\right)^2\rho(E_l)\,. \tag{A3}$$

The second factor in the argument of Eq. (A3), the dipole matrix element between Bloch states, can be developed as follows:

$$\int u^*_{l,\vec{k}}(\vec{r})e^{-i\vec{k}\cdot\vec{r}}(-i\hbar\vec{\nabla})u_{c,\vec{k}}(\vec{r})e^{i\vec{k}\cdot\vec{r}}d^3r = \int u^*_{l,\vec{k}}(\vec{r})(-i\hbar\vec{\nabla})u_{c,\vec{k}}(\vec{r})d^3r + \hbar\vec{k}\int u^*_{l,\vec{k}}(\vec{r})u_{c,\vec{k}}(\vec{r})d^3r\,. \tag{A4}$$

If l denotes an s-like state, i.e., we have photoionization, the first integral in Eq. (A4) will vanish, to zeroth order in k, while the second is finite for $l = c$. Consequently we end up with a term proportional to $\hbar k$, a forbidden dipole transition.

In the case of photoneutralization, l is a valence-band state (of mainly p character) and in this case the first integral in Eq. (A4) is finite and the second vanishes (for small $\vec{k}$). This gives a constant term independent of $\vec{k}$, an allowed transition.

The first factor inside Eq. (A3) can be expressed as

$$A_D(\vec{k}_c) = -\langle c,\vec{k}|U_D|\psi_D\rangle/(E_c(\vec{k}) + |E_D|)\,. \tag{A5}$$

This results from application of the one-electron Schrödinger equation to Eq. (A1) with the impurity potential U_D, and describes the admixture of (conduction) band states into the donor state.

To evaluate properly the matrix element in the numerator we must know the continuum Bloch state. We will make rough estimates of this matrix element for a few cases.

A. Extended potential

Example: $U_D \propto -e^2/r$, i.e., a Coulomb potential. If we use plane waves instead of Bloch states, the matrix element can be expressed as

$$\langle|U_D|\rangle \propto \int e^{-i\vec{k}\cdot\vec{r}}\left(-\frac{e^2}{r}\right)e^{-\alpha r}d^3r = \frac{4\pi e^2}{\alpha^2+k^2}\,. \tag{A6}$$

Using the full Bloch state, and expanding the periodic part $u_{\vec{k}}(\vec{r})$ in the reciprocal-lattice vectors gives

$$u^*_{\vec{k}}(\vec{r}) = \sum_{\vec{G}} C(\vec{G}-\vec{k})e^{i\vec{G}\cdot\vec{r}}\,, \tag{A7a}$$

i.e., for small k:

$$u^*_0(r) = \sum_{\vec{G}} C_{\vec{G}}e^{i\vec{G}\cdot\vec{r}}\,. \tag{A7b}$$

Consequently,

$$\langle |U_D| \rangle \propto \int u_k^*(r) e^{-i\vec{k}\cdot\vec{r}} \left(-\frac{e^2}{r}\right) e^{-\alpha r} d^3r$$

$$\approx \sum_{\vec{G}} C_{\vec{G}} \int e^{i(\vec{G}-\vec{k})\cdot\vec{r}} \left(-\frac{e^2}{r}\right) e^{-\alpha r} d^3r$$

$$= \sum_{\vec{G}} C_{\vec{G}} \frac{4\pi e^2}{\alpha^2 + (\vec{G}-\vec{k})^2} . \quad \text{(A8)}$$

This means that, although the number of $C_{\vec{G}}$'s needed in Eq. (A7) to describe $u_0(r)$ might be considerable, it is probably sufficient to retain only very few terms in Eq. (A8) because of the denominator $\propto [\alpha^2 + (\vec{G}-\vec{k})^2]$. E.g., for $E_D \approx 0.1$ eV, $\alpha^2 = [(2m^* E_t)/\hbar^2] \approx 4 \times 10^{17}\ (m^{-2})$ while for the first $\vec{G} \neq 0$, $(\vec{G}_1 - \vec{k})^2 \approx [(2\pi/a)(\sqrt{3}/2)]^2 \approx 1 \times 10^{20}\ (m^{-2})$. This means that the $\vec{G}=0$ term is favored compared to $\vec{G}_1$ by a factor $\gtrsim 100$. Therefore, keeping only the $\vec{G}=0$ term, we get

$$A_D(\vec{k}) \propto \alpha^{5/2}/(\alpha^2 + k^2)^2 . \quad \text{(A9)}$$

B. Localized potential

Example: A square-well potential with depth $|V_0|$ for $r < r_0$:

$$\langle |U_D| \rangle \propto \int u_{\vec{k}}^*(r) e^{-i\vec{k}\cdot\vec{r}} V(\vec{r}) \psi_D d^3r$$

$$\underset{\vec{k}\cdot\vec{r}_0 \ll 1}{\approx} V_0 \int_{\Omega(r<r_0)} u_{\vec{k}}^*(\vec{r}) \psi_D \, d^3r . \quad \text{(A10)}$$

For small $\vec{k}$ we get

$$u_{\vec{k}}(\vec{r}) = u_0(\vec{r}) + \vec{k} \cdot \vec{\nabla}_{\vec{k}} u_{\vec{k}}(\vec{r}) + \cdots . \quad \text{(A11)}$$

When $u_{\vec{k}}$ and ψ_D have the same symmetry the first term will dominate and give an (almost) constant matrix element near the Γ point. Hence, from Eq. (A5) we get for a localized potential

$$A_D(\vec{k}) \propto \alpha^{1/2}/(\alpha^2 + k^2) . \quad \text{(A12)}$$

If, however, $u_0(r)$ and ψ_D have different symmetry, the integral vanishes and we must use the term proportional to $\vec{k}$ in Eq. (A11), making the matrix element proportional to $\vec{k}$.[53]

SUMMARY

For an s-like donor state composed of conduction-band states through a localized potential, we can write the ionization cross section

$$\sigma_n^0(h\nu) \propto \frac{1}{h\nu} A_D^2(\vec{k}) \vec{k}^2 \rho_c(h\nu - E_D) \propto \frac{\sqrt{E_D}(h\nu - E_D)^{3/2}}{(h\nu)^3} , \quad \text{(A13)}$$

and for the neutralization cross section we get

$$\sigma_p^0(h\nu) \propto \frac{1}{h\nu} A_D^2(\vec{k} = [2m_v^*(h\nu - E_T)]^{1/2}/\hbar) \rho_v(h\nu - E_T)$$

$$\propto (E_D^\Gamma)^{1/2}(h\nu - E_T)^{1/2} \Big/ h\nu \left(E_D^\Gamma + \frac{m_v^*}{m_c^*}(h\nu - E_T)\right)^2 , \quad \text{(A14)}$$

where we have use parabolic bands and put $E_T = E_g - E_D$. E_D^Γ is the binding energy measured from the (conduction-band) Γ minimum.

APPENDIX B: DISCRETE METHOD FOR DECONVOLUTION OF CC PHONON-ASSISTED OPTICAL SPECTRA

Assume that we have an experimental low-temperature spectral distribution $\sigma_T(x)$ (where x corresponds to $h\nu$), which e.g., can be an absorption spectrum. If N linear CC modes are present with energies $\hbar\omega_i = \Delta x_i$ and coupling strengths λ_i, we can express $\sigma_T(x)$ as

$$\sigma_T(x) = e^{-\Lambda} \sum_{M_1=0}^{\infty} \cdots \sum_{M_N=0}^{\infty} \left[\left(\prod_{i=1}^{N} \frac{(\lambda_i)^{M_i}}{(M_i)!} \right) \times \sigma_{el}\left(x - x_0 - \sum_{i=1}^{N} M_i \Delta x_i\right) \right] \quad \text{(B1)}$$

in agreement with Sec. II, Eq. (9). Here σ_{el} denotes the electronic part of the cross section to be determined as a function of x and $\Lambda = \sum_{i=1}^{N} \lambda_i$. Assume we select experimental values at $x = x_0 + k\Delta x$, where $k = 0, 1, 2, \ldots, T$.

We let $\Delta x_i = \alpha_i \Delta x$, where α_i are integers, and assume that $\sigma_T(x) = 0$ for $x < x_0$, which is indeed what happens in the real case for low temperatures, where x_0 is the pure electronic edge. Let

$$Y_k = \sigma_T(x_0 + k\Delta x) \quad \text{(B2)}$$

and

$$\sigma_k = \sigma_{el}(x_0 + k\Delta x). \quad \text{(B3)}$$

From Eq. (B1) follows:

$$Y_k = e^{-\Lambda} \sum_{M_1=0}^{\infty} \cdots \sum_{M_N=0}^{\infty} \left[\left(\prod_{i=1}^{N} \frac{(\lambda_i)^{M_i}}{(M_i)!} \right) \sigma_{k - \sum_i \alpha_i M_i} \right] . \quad \text{(B4)}$$

This equation is solved for σ_k by using Z transforms.[93] For this we define the following Z transforms related to expression (B4):

$$Y(Z) = \sum_{k=0}^{\infty} Y_k Z^k , \quad \text{(B5)}$$

$$H_i(Z) = e^{-\lambda_i} \sum_{M_i=0}^{\infty} \frac{(\lambda_i)^{M_i}}{(M_i)!} Z^{M_i}$$

$$= e^{\lambda_i (Z-1)} \quad \text{for } i = 1, \ldots, N, \quad \text{(B6)}$$

$$S(Z)=\sum_{k=0}^{\infty}\sigma_k Z^k. \tag{B7}$$

Substituting Eq. (B4) in Eq. (B5), we obtain

$$Y(Z)=e^{-\Lambda}\prod_{i=1}^{N}\left(\sum_{M_i=0}^{\infty}\frac{(\lambda_i)^{M_i}}{(M_i)!}\right)\sum_k \sigma_{k-\sum_i\alpha_i M_i}Z^k$$

$$=e^{-\Lambda}\prod_{i=1}^{N}\left(\sum_{M_i=0}^{\infty}\frac{(\lambda_i)^{M_i}}{(M_i)!}Z^{\alpha_i M_i}\right)$$

$$\times\sum_k \sigma_{k-\sum_i\alpha_i M_i}Z^{k-\sum_i\alpha_i M_i}. \tag{B8}$$

Since the α_i are integers, the sum over k is independent of $\sum_i\alpha_i M_i$, and one can factor the summations, giving

$$Y(Z)=S(Z)\prod_{i=1}^{N}H_i(Z^{\alpha_i}). \tag{B9}$$

Thus, we obtain

$$S(Z)=F(Z)Y(Z), \tag{B10}$$

where

$$F(Z)=1/\Pi_i H_i(Z^{\alpha_i})=e^{\Lambda-\sum_i\lambda_i Z^{\alpha_i}}. \tag{B11}$$

Formally we can now write the solution to Eq. (B4) as

$$\sigma_k=\sum_{j=0}^{\infty}f_j Y_{k-j}, \tag{B12}$$

where the f_j's are the coefficients in the expansion

$$F(Z)=\sum_{j=0}^{\infty}f_j Z^j. \tag{B13}$$

To find an expression for the coefficients f_j in this expansion we note that according to Eq. (B11),

$$F(Z)=e^{\Lambda}\sum_{M_1=0}^{\infty}\cdots\sum_{M_N=0}^{\infty}\left[\left(\prod_{i=1}^{N}\frac{(-\lambda_i)^{M_i}}{(M_i)!}\right)Z^{\sum_i\alpha_i M_i}\right]. \tag{B14}$$

With the aid of these equations, we can now identify the coefficients f_j in Eq. (B12) simply by inspection:

$$f_j=e^{\Lambda}\sum_{M_1,\ldots,M_N}\left[\prod_{i=1}^{N}\left(\frac{(-\lambda_i)^{M_i}}{(M_i)!}\right)\right], \tag{B15}$$

where the sum goes over all combinations of the M_i's, such that $\sum_i\alpha_i M_i=j$.

The deconvolved spectrum can thus be computed from Eq. (B12) with the f_j from Eq. (B15). If the spacing Δx between the experimental points is chosen much smaller than the phonon energies (in our case we used $\Delta x=1$ meV whereas phonon energies were of the order of 20–50 meV), most of the coefficients in Eq. (B14) are identically zero. For calculation of f_j it may sometimes be convenient to use a recursion relation. This can be derived in the following way.

Differentiating (B11), we get

$$\frac{dF}{dZ}(Z)=F(Z)\left(-\sum_i\lambda_i\alpha_i Z^{\alpha_i-1}\right),$$

into which we can substitute (B13) for $F(Z)$ to give

$$\sum_{j=1}^{\infty}jf_j Z^{j-1}=\sum_i\sum_{j=0}^{\infty}(-\lambda_i\alpha_i)f_j Z^{j+\alpha_i-1}.$$

Replacing the index of summation j by $j-\alpha_i$, for each i on the right, and equating coefficients of like powers of Z^{j-1}, we obtain

$$f_j=\frac{-e^{\Lambda}}{j}\sum_{i=1}^{N}\lambda_i\alpha_i f_{j-\alpha_i}, \tag{B16}$$

which is to be used with the starting values

$$f_j=0,\quad j<0,$$

$$f_0=e^{\Lambda},$$

$$f_j=0,\quad 0<j<\min\{\alpha_i\}_i.$$

If we again note that $f_j\neq 0$ only for $j=\sum_i\alpha_i M_i$, where α_i and $\{M_i\}$ are integers, we can rewrite the recursion relation so that only the nonzero f_j are computed

$$f_j=f_{\sum_i\alpha_i M_i}=\frac{-e^{\Lambda}}{j}\sum_i\lambda_i\alpha_i f_{j-\alpha_i}. \tag{B17}$$

For the special case where two phonon modes are active, the recursion formula corresponding to Eq. (B15) will read

$$f_k=\frac{-e^{\lambda_1+\lambda_2}}{k}(\lambda_1\alpha_1 f_{k-\alpha_1}+\lambda_2\alpha_2 f_{k-\alpha_2}). \tag{B18}$$

APPENDIX C: QUANTITATIVE DISCUSSION ON EXCITATION AND RECOMBINATION KINETICS IN GaP:O

A. PLE measurements

The proper application of this technique to measure σ_{p1}^0 in p-type O-doped GaP is dependent on the validity of Eq. (13), i.e., several terms in Eq. (12) have to be negligibly small compared to the leading term $\sigma_{p1}^0 N_T^+ I$. The occupation of the O donor, i.e., N_T^0 is determined by the recombination rates of these photoexcited donors with holes (free or bound to acceptors) which can occur radiatively or nonradiatively via Auger processes.[94] The maximum lifetime τ_d observed for electrons on the donor under these circumstances is about 5×10^{-5} sec.[60,94,95] With a typical excitation intensity I

$\approx 10^{14}$ photons/cm^2 sec, $N_T^+ \approx N_T \approx 10^{16}$ cm^{-3}, and cm^{-3}, and $\sigma_{p1}^0 \approx 10^{-16}$ cm^2, we obtain an excitation rate $U_1 = N_T^+ \sigma_{p1}^0 I \approx 10^{14}$ cm^{-3} sec^{-1}. A conservative maximum value of N_T^0 is therefore obtained as $N_T^0 \approx U_i \tau_d = 5 \times 10^9$ cm^{-3}. Thus, $N_T^0/N_T^+ < 10^{-6}$ (for all temperatures below room temperature), which means the term $(\sigma_{n1}^0 + \sigma_{p2}^0) N_T^0 I$ in Eq. (12) can be safely neglected. The two-electron state has a lifetime $\tau_2 \approx 10^{-9}$ sec in p-type GaP.[22] If we assume a maximum excitation rate U_2 for the two-electron state, we obtain $U_2 \approx 10^{14} \times 5 \times 10^9 \times 10^{-16} \approx 5 \times 10^7$ cm^{-3} sec^{-1}, which means $N_{T2} \approx U_2 \tau_2 < 1$ cm^{-3}. Thus, all two-electron processes can also be ignored in Eq. (12). This already means that the spectral behavior of σ_{p1}^0 measured by PLE spectra is safe [Eq. (13)]. The background observed in the experiment (above dark current in the photomultiplier) is due to the two terms $c_{p2} N_{T2} + c_{n1} N_T^+$. We just showed that the first one is negligibly small. The excitation rate U_n for electrons via O in p-GaP can be obtained as $U_n = N_T^0 \sigma_{n1}^0 I < 5 \times 10^9 \times 10^{-16} \times 10^4 = 5 \times 10^7$ cm^{-3} sec^{-1}. The minority electron lifetime τ_n in p-type GaP:O is estimated as $\tau_n \leq 10^{-6}$ sec for $T < 300$ K,[95] which means we are dealing with an electron concentration $n \approx U_n \tau_n \approx 50$ cm^{-3} for excitation via the O center alone. Two-step excitations via other centers present in the material could conceivably raise this value, but probably not more than a couple of orders of magnitude, since the occupation of such centers must also be low in p-GaP. Thus, $c_{n1} N_T^+ = \sigma_{n1} n v_n N_T^+ < 10^{-17} \times 10^3 \times 10^7 \times 10^{16} = 10^9$ cm^{-3} sec^{-1}, about five orders of magnitude smaller than the leading term $N_T^+ \sigma_{p1}^0 I$. Thus, the background should be negligibly small below 300 K, in agreement with experimental observations.

There is one problem that is not apparent in the above treatment, but does show up in experiment, namely the effect of relative donor-acceptor pair distributions on excitation processes. At low temperatures the free-hole concentration is so low that donor-acceptor pair recombination (radiative or nonradiative Auger) is the dominating mechanism that governs the occupation of oxygen centers. The maximum lifetime (5×10^{-5} sec) given above refers to luminescence data, but there are O centers which are situated so far from acceptors that they have an extremely small probability for recombination, but they may well be active in excitation processes. Therefore the total steady-state concentration of occupied donors may be much larger than calculated above, which would influence the two-step excitation of minority electrons in the conduction band via O. That this occurs in practice is proved by the remarkably strong (green) shallow DA-pair emission observed for $T \lesssim 50$ K with two-step excitation via O in GaP. As long as N_T^0 for these O centers that do not effectively take part in the recombination process is not raised to be comparable to N_T^+, Eq. (13) will still be valid. Since N_T^0 and N_{T2} depend on I, a deviation from a linear dependence of L on I would occur if any of the terms except $\sigma_{p1}^0 N_T^+ I$ in Eq. (12) were not negligible. As seen from Fig. 6 perfect linearity is observed in our experiments, therefore, Eq. (13) is indeed valid. [Since the green DA-pair emission varies with (below band gap) intensity as $\approx I^{1.4}$, a PLE spectrum based on detection of the green emission does not give a straightforward measurement of $\sigma_{p1}^0(h\nu)$.]

B. PLQ measurements

The most sensitive sets of measurements were here performed on n-type O-doped material, having rather high resistivity even at room temperature (the thermal equilibrium Fermi level was found to be situated about 0.75 eV below the conduction band from Hall data). Therefore omitting the two-electron state in the analysis would seem to be a serious limitation. The terms that are omitted in Eq. (17) are, of course, the same as those included in Eq. (12), and there is no difficulty in principle to include them in Eq. (17), except for a much more complicated final expression. The most important terms involved are $\sigma_{n2}^0 N_{T2} I_s$, $\sigma_{p2}^0 N_T^0 I_s$, and $c_{p2} N_{T2}$, which are all very small under the conditions of the experiments. The position of the two-electron level is not established, but from data for the optical cross sections[22,62] one can find that σ_{n2}^0 and σ_{p2}^0 are both very small at low temperature in the region $0.8 < h\nu < 1.4$ eV, where our measurements were performed. The thermal capture term $c_{p2} N_{T2}$ is small simply because p is very small. Therefore, proper inclusion of the two-electron state will not influence the analysis of our PLQ data for O in GaP according to Eq. (20).

[1] R. L. Aggarwal and A. K. Ramdas, Phys. Rev. 140, A1246 (1965).
[2] D. G. Thomas, M. Gershenzon, and F. A. Trumbore, Phys. Rev. 133, A269 (1964).
[3] P. J. Dean, R. A. Faulkner, S. Kimura, and M. Ilegems, Phys. Rev. B 4, 1926 (1971).
[4] S. T. Pantelides, Festkörperprobleme 15, 149 (1975).
[5] P. J. Dean, C. H. Henry, and C. J. Frosch, Phys. Rev. 168, 812 (1968).
[6] P. J. Dean, J. Lumin. 1-2, 398 (1970); 7, 51 (1973).
[7] T. N. Morgan, J. Lumin. 1, 420 (1970); 2, 420 (1970).
[8] P. J. Dean, W. Shairer, M. Lorenz, and T. N. Morgan,

J. Lumin. 9, 343 (1974).
[9]T. N. Morgan, B. Welber, and R. N. Bhargava, Phys. Rev. 166, 751 (1968).
[10]C. H. Henry, P. J. Dean, and J. D. Cuthbert, Phys. Rev. 166, 754 (1968).
[11]J. M. Dishman and M. DiDomenico, Phys. Rev. B 4, 2621 (1971); B 6, 683 (1972).
[12]H. J. Queisser, Festkörperprobleme 15, 45 (1971).
[13]M. Blätte and F. Willman, Opt. Commun. 4, 178 (1971).
[14]W. H. Koschel, S. G. Bishop, and B. D. McCombe, Solid State Commun. 19, 521 (1976).
[15]H. J. Stocker and M. Schmidt, J. Appl. Phys. 47, 2450 (1976).
[16]R. A. Chapman and W. G. Hutchinson, Phys. Rev. Lett. 18, 443 (1967).
[17]W. J. Brown, Jr., D. A. Woodbury, and J. S. Blakemore, Phys. Rev. B 8, 5664 (1973).
[18]W. Schairer and M. Schmidt, Phys. Rev. B 10, 2501 (1974).
[19]D. Bois and P. Pinard, Phys. Rev. B 9, 4171 (1974).
[20]G. Lucovsky, Solid State Commun. 3, 299 (1965).
[21]H. B. Bebb, Phys. Rev. 185, 1116 (1969).
[22]H. Kukimoto, C. H. Henry, and F. R. Merritt, Phys. Rev. B 7, 2486 (1973).
[23]J. I. Pankove, *Optical Processes in Semiconductors* (Prentice-Hall, New York, 1971), p. 139ff.
[24]A. T. Vink, Ph.D. thesis (Eindhoven, 1974) (unpublished).
[25]E. W. Williams, Brit. J. Appl. Phys. 18, 253 (1967).
[26]K. Huang and A. Rhys, Proc. R. Soc. A 204, 406 (1950).
[27]M. Lax, J. Chem. Phys. 20, 1752 (1952).
[28]D. L. Dexter, Solid State Phys. 6, 353 (1958).
[29]J. J. Markham, Rev. Mod. Phys. 31, 956 (1959).
[30]T. H. Keil, Phys. Rev. A 140, 601 (1965).
[31]C. S. Kelley, Phys. Rev. B 6, 4112 (1972).
[32]J. J. Hopfield, J. Phys. Chem. Solids 10, 110 (1958).
[33]U. Lindefelt (unpublished).
[34]W. Kohn, Solid State Phys. 5, 257 (1957).
[35]W. Dumke, Phys. Rev. 132, 1998 (1963).
[36]D. M. Eagles, J. Phys. Chem. Solids 16, 76 (1960).
[37]E. T. Copson, *Functions of a Complex Variable* (Oxford, London, 1935), p. 270.
[38]D. K. Brice, Phys. Rev. 188, 1280 (1969).
[39]K. Era, S. Shionoya, Y. Washizawa, and H. Ohmatsu, J. Phys. Chem. Solids 29, 1843 (1968).
[40]B. Monemar and L. Samuelson, J. Lumin. 12, 507 (1976); 13, 507 (1976).
[41]L. Samuelson and B. Monemar, following paper, Phys. Rev. B 18, 830 (1978).
[42]R. Olsson, Phys. Status Solidi B 46, 299 (1971).
[43]C. T. Sah, L. Forbes, L. L. Rosier, and A. F. Tasch, Jr., Solid State Electron. 13, 759 (1970).
[44]G. Björklund and H. G. Grimmeiss, Solid State Electron. 14, 589 (1971).
[45]A. F. Tasch, Jr. and C. T. Sah, Phys. Rev. B 1, 800 (1970).
[46]C. H. Henry, J. Lumin. 7, 127 (1973).
[47]C. H. Henry, J. Electron. Mater. 4, 1037 (1975).
[48]D. V. Lang, J. Appl. Phys. 45, 3014 (1974); 45, 3023 (1974).
[49]D. V. Lang and R. A. Logan, J. Electron. Mater. 4, 1053 (1975).
[50]S. Braun and H. G. Grimmeiss, J. Appl. Phys. 45, 2658 (1974).
[51]S. Braun and H. G. Grimmeiss, Solid State Commun. 12, 657 (1973).
[52]C. H. Henry and D. V. Lang, Proceedings of the Twelfth International Conference on Physics and Semiconductors, Stuttgart, 1974 (unpublished), p. 411.
[53]H. G. Grimmeiss, L.-Å. Ledebo, C. Ovrén, and T. N. Morgan, in Ref. 52, p. 386.
[54]A. L. Lin, E. Omelianovski, and R. H. Bube, J. Appl. Phys. 47, 1852 (1976).
[55]A. L. Lin and R H. Bube, J. Appl. Phys. 47, 1859 (1976).
[56]H. G. Grimmeiss and L.-Å. Ledebo, J. Appl. Phys. 46, 2155 (1975).
[57]D. C. Wong and C. M. Penchina, Appl. Phys. Lett. 25, 466 (1974).
[58]B. Monemar, Phys. Rev. B 8, 5711 (1973).
[59]B. Monemar, Phys. Rev. B 10, 676 (1974).
[60]C. H. Henry, H. Kukimoto, G. L. Miller, and F. R. Merritt, Phys. Rev. B 7, 2499 (1973).
[61]H. G. Grimmeiss and B. Monemar, Phys. Status Solidi A 19, 505 (1973).
[62]C. H. Henry (private communication); and C. H. Henry and D. V. Lang, Phys. Rev. B 15, 989 (1977).
[63]P. J. Dean and D. C. Herbert, J. Lumin. 14, 55 (1976).
[64]P. J. Dean and C. H. Henry, Phys. Rev. 176, 928 (1968).
[65]B. Monemar and L. Samuelson, Proceedings of the Thirteenth International Conference on Physics and Semiconductors, Rome, 1976 (unpublished), p. 639.
[66]C. Ovrén (private communication).
[67]W. W. Anderson, Solid State Electron. 18, 235 (1975).
[68]Yu. I. Zavadskii and B. K. Kornilov, Phys. Status Solidi 42, 617 (1970).
[69]H. Kukimoto, S. Shionoya, T. Koda, and R. Hioki, J. Phys. Chem. Solids 29, 935 (1968).
[70]W. J. Brown, Jr., and J. S. Blakemore, J. Appl. Phys. 43, 2242 (1972).
[71]H. B. Bebb and R. A. Chapman, J. Phys. Chem. Solids 28, 2087 (1967).
[72]J. M. Herman III and C. T. Sah, J. Appl. Phys. 44, 1259 (1973).
[73]A. A. Kopylov and A. N. Pikhtin, Sov. Phys.-Semicond. 8, 1563 (1975).
[74]K. K. Rebane, *Impurity of Solids* (Plenum, New York, 1970).
[75]A. S. Barker, R. Berman, and H. W. Verleur, J. Phys. Chem. Solids 34, 123 (1973).
[76]T. Arai, N. Asanuma, K. Kudo, and S. Umemoto, Jpn. J. Appl. Phys. 11, 206 (1972).
[77]C. H. Henry and D. V. Lang, Phys. Rev. Lett. 35, 1525 (1975).
[78]T. N.Morgan, Phys. Rev. Lett. 21, 819 (1968).
[79]H. G. Grimmeiss, Ann. Rev. Mater. Sci. 7, 341 (1977).
[80]D. V. Lang and M. Jaros (unpublished).
[81]A. Onton, Phys. Rev. 186, 786 (1969).
[82]A. T. Vink, R. L. A. van der Heyden, and J. A. van der Does de Bye, J. Lumin. 8, 105 (1972).
[83]A. C. Carter, P. J. Dean, M. S. Skolnick, and R. A. Stradling (unpublished).
[84]A. A. Kopylov and A. N. Pikhtin, Sov. Phys.-Semicond. 11, 510 (1977).
[85]P. J. Dean and D. G. Thomas, Phys. Rev. 150, 690 (1966).
[86]N. O. Lipari and M. Altarelli, Phys. Rev. B 15, 4883 (1977).

[87]W. Berndt, A. A. Kopylov, and A. N. Pikhtin, JETP Lett. 22, 284 (1975).
[88]R. A. Street and W. Senske, Phys. Rev. Lett. 37, 1292 (1976).
[89]L. L. Chase, W. Hayes, and J. F. Ryan, Solid State Phys. 10, 2957 (1977).
[90]E. O. Kane, *Semiconductors and Semimetals*, edited by R. K. Willardson and R. C. Beer (Academic, New York, 1966), Vol. 1, p. 75.
[91]T. N. Morgan and L. Samuelson (unpublished).
[92]This description is in terms of real impurity wave functions ψ_D. A pseudo-effective-mass treatment as used by Pantelides (Ref. 4) would give results similar to these except with ψ_D replaced by φ_D, the pseudo wave function in the equations below. This is because the core orthogonalization terms give only small contributions to the matrix elements entering the Golden Rule formulas; J. Bernholc (private communication).
[93]For an introduction to Z-transform methods to solve difference equations, see, e.g., E. J. Jury, *Theory and Application of the Z-transform Method* (Wiley, New York, 1964).
[94]J. M. Dishman, Phys. Rev. B 3, 2588 (1971).
[95]J. S. Jayson, R. Z. Bachrach, P. D. Dapkus, and N. E. Schumaker, Phys. Rev. B 6, 2357 (1972).